

ANALYSIS OF DUAL-POLARIZED APERTURE-COUPLED MICROSTRIP
ANTENNAS WITH H-SHAPED SLOTS AND EQUIVALENT CIRCUIT
MODELING OF H-SHAPED SLOTS

A THESIS SUBMITTED TO
THE GRADUATE SCHOOL OF NATURAL AND APPLIED SCIENCES
OF
MIDDLE EAST TECHNICAL UNIVERSITY

BY

KADİR İŞERİ

IN PARTIAL FULFILLMENT OF THE REQUIREMENTS
FOR
THE DEGREE OF MASTER OF SCIENCE
IN
ELECTRICAL AND ELECTRONICS ENGINEERING

JULY 2012

Approval of the thesis:

**EQUIVALENT CIRCUIT MODELING OF APERTURE-COUPLED
MICROSTRIP ANTENNAS**

submitted by **KADİR İŞERİ** in partial fulfillment of the requirements for the degree of **Master of Science in Electrical and Electronics Engineering Department, Middle East Technical University** by,

Prof. Dr. Canan Özgen _____
Dean, Graduate School of **Natural and Applied Sciences**

Prof. Dr. İsmet Erkmek _____
Head of Department, **Electrical and Electronics Engineering**

Assoc. Prof. Dr. Lale Alatan _____
Supervisor, **Electrical and Electronics Engineering Dept., METU**

Examining Committee Members:

Prof. Dr. S. Sencer Koç _____
Electrical and Electronics Engineering Dept., METU

Assoc. Prof. Dr. Lale Alatan _____
Electrical and Electronics Engineering Dept., METU

Prof. Dr. Altunkan Hızal _____
Electrical and Electronics Engineering Dept., METU

Prof. Dr. Mustafa Kuzuoğlu _____
Electrical and Electronics Engineering Dept., METU

M.Sc. Şakir Karan _____
ASELSAN A.Ş.

Date: _____ 13 July 2012

I hereby declare that all information in this document has been obtained and presented in accordance with academic rules and ethical conduct. I also declare that, as required by these rules and conduct, I have fully cited and referenced all material and results that are not original to this work.

Name, Last name : Kadir İŞERİ

Signature :

ABSTRACT

ANALYSIS OF DUAL-POLARIZED APERTURE-COUPLED MICROSTRIP ANTENNAS WITH H-SHAPED SLOTS AND EQUIVALENT CIRCUIT MODELING OF H-SHAPED SLOTS

İşeri, Kadir

M. Sc., Department of Electrical and Electronics Engineering

Supervisor: Assoc. Prof. Dr. Lale Alatan

July 2012, 80 pages

This thesis includes the design, production and measurement of a wideband dual-polarized X-band aperture-coupled microstrip patch antenna. The wideband and dual-polarized operation is achieved through the use of H-shaped coupling slots. Therefore, the equivalent circuit modeling of a microstrip line fed H-shaped slot is also studied in this thesis. A step-by-step procedure is followed during the design process of the dual-polarized aperture-coupled microstrip antenna. First, an aperture-coupled microstrip antenna with a single rectangular slot, that exhibits a wideband characteristic for single polarization, is designed. Then, the design procedure is repeated for an antenna with H-shaped slot in order to satisfy the same specifications with a shorter slot. Finally, dual-polarized aperture-coupled microstrip antenna is designed. At this configuration, two H-shaped slots are used and they are placed orthogonal to each other. During the design process, the effects of antenna parameters on the input impedance characteristics of the antenna are investigated. These parametric analyses are done in CST Microwave Studio[®]. The

designed dual-polarized wideband aperture-coupled microstrip antenna is manufactured. Simulation results and measurement results are compared.

During the equivalent circuit modeling of an H-shaped slot fed by a microstrip line, an approach based on the reciprocity theorem is utilized. The method was originally proposed for rectangular shaped slots, in this thesis it is generalized for arbitrarily shaped slots. Software codes are developed in MATLAB to calculate the equivalent impedance of the slot.

Keywords: Patch antenna, aperture-coupled microstrip antenna, dual-polarized aperture-coupled microstrip antenna, H-shaped slotted microstrip antenna.

ÖZ

ÇİFT KUTUPLU VE H-TİPİ YARIKLI YARIK BAĞLAŞIMLI MİKROŞERİT ANTEN ANALİZLERİ VE H-TİPİ YARIKLARIN DEVRE ŞEKLİNDE MODELLEMESİ

İşeri, Kadir

Yüksek Lisans, Elektrik ve Elektronik Mühendisliği Bölümü

Tez Yöneticisi: Doç. Dr. Lale Alatan

Temmuz 2012, 80 sayfa

Bu tez geniş band çift kutuplu X-band yarık bağlaşımlı mikroşerit anten tasarımını, üretimini ve mikroşerit hat ile beslenen H-tipi yarığın eş devre modellenmesini içerir. Tasarım kısmında yarık bağlaşımlı mikroşerit anten adım adım geliştirilmiştir. İlk olarak, dikdörtgen şeklindeki yarık kullanılarak yarık bağlaşımlı mikroşerit anten tasarlanmıştır. Sonraki aşamada H-tipi yarık kullanılan yarık bağlaşımlı mikroşerit anten tasarımı gerçekleştirilmiştir ve bu tip antenin gerekli anten parametrelerine olan etkisi incelenmiştir. En son aşamada ise çift kutuplu yarık bağlaşımlı mikroşerit anten tasarımı gerçekleştirilmiştir. Bu konfigürasyonda iki adet H-tipi yarık birbirlerine dik olacak şekilde yerleştirilmiştir. Tasarım aşamasında anten parametrelerinin antenin giriş empedansına olan etkileri incelenmiştir. Parametrik analizler CST Microwave Studio® benzetim programında yapılmıştır. Tasarım aşaması bittikten sonra çift kutuplu ve geniş bantlı yarık bağlaşımlı mikroşerit anten üretilmiştir. Bu aşamada üretilen anten ile benzetim programında tasarlanan antenler karşılaştırılmıştır.

Ek olarak, mikroşerit hat ile beslenen H-tipi yarığın eş devre modellemesi üzerinde çalışılmıştır. Modelleme aşamasında karşılıklılık teoremi kullanılmıştır. Modelleme sırasında yarık üçgen ağlara bölünmüştür ve her ağ üzerindeki akım değerleri hesaplanmıştır. Sonraki aşamada modelleme sırasında kullanılan integral denklemlerinin doğruluğunu kontrol etmek için dipolün karşılıklı ve kendi empedansı hesaplanmıştır. Tüm modelleme sırasındaki analizler MATLAB programında yapılmıştır ve son olarak dikdörtgen ve H-tipi yarıkların empedansları hesaplanmış ve benzetim programı sonuçları ile karşılaştırılmıştır.

Anahtar kelimeler: Yama anten, yarık bağlaşımlı mikroşerit anten, çift kutuplu yarık bağlaşımlı mikroşerit anten, H-tipi yarıklı mikroşerit anten.

To My Dear Family

ACKNOWLEDGEMENTS

I would like to express my sincere gratitude to my supervisor Assoc. Prof. Dr. Lale Alatan for her guidance, advice, criticism, patience and help. I would also like to thank Prof Dr. Altunkan Hızal, Prof Dr. S. Sencer Koç, Prof. Dr. Mustafa Kuzuoğlu and Şakir Karan being in my jury and sharing their opinions.

I would also like to thank ASELSAN A.Ş. for the help on the production and measurement stage of the antenna.

Firstly, I would like to thank plentifully to my family for their care and support.

At the writing period of the thesis, I could not deny to the support of my colleagues. I want to thank them all for encouraging me to complete this thesis. Firstly, I want to thank especially to Egemen Yıldırım for his helpful behaviors and useful point of views. Then, I want to thank to Gökhan Yılmaz, Ferdi Karaduman, Fatih İzçiler, Utku Kaba, Ahmet Muaz Ateş, Görkem Akgül, Damla Duygu Tekbaş and Hüsnü Erdöşemeci.

TABLE OF CONTENTS

ABSTRACT.....	iv
ÖZ.....	vi
ACKNOWLEDGEMENTS.....	viii
TABLE OF CONTENTS.....	x
LIST OF TABLES.....	xii
LIST OF FIGURES.....	xiii
CHAPTERS	
1.INTRODUCTION.....	1
2.APERTURE- COUPLED MICROSTRIP ANTENNAS.....	8
3.PARAMETRIC STUDY OF APERTURE-COUPLED MICROSTRIP ANTENNAS.....	13
3.1 Introduction.....	13
3.2 Analysis at the Design of an Aperture-Coupled Microstrip Antenna with a Single Rectangular Slot.....	14
3.2.1 Parameters used in the Aperture-Coupled Microstrip Antenna Design with a Single Rectangular Slot.....	15
3.2.2 The Parametrical Analysis on the Length of the Microstrip Patch.....	16
3.2.3 The Parametrical Analysis on the Length of the Slot on the Aperture.....	18
3.2.4 The Parametrical Analysis on the Width of the Slot on the Aperture.....	19
3.2.5 The Parametrical Analysis on the Thickness of the Patch Substrate.....	21
3.2.6 The Parametrical Analysis on the Length of the Stub.....	22
3.2.7 The Parametrical Analysis regarding the Displacement of the Slot in x-Direction.....	24

3.2.8 The Parametrical Analysis regarding the Displacement of the Slot in y-Direction	25
3.3 Analysis on the Design of an Aperture-Coupled Microstrip Antenna with a Single H-Shaped Slot.....	28
3.3.1 Parameters used in the Aperture-Coupled Microstrip Antenna Design with a Single H-Shaped Slot.....	28
3.3.2 The Parametrical Analysis on the Stub Length	30
3.3.3 The Parametrical Analysis on the Length of the Center Slot.....	31
3.3.4 The Parametrical Analysis on the Width of the Center Slot.....	33
3.3.5 The Parametrical Analysis on the Length of the Slot Edge.....	34
3.3.6 The Parametrical Analysis on the Width of the Slot Edge.....	35
3.4 Analyses on the Design of a Dual-Polarized Aperture-Coupled Microstrip Antenna with H-Shaped Slots.....	40
4.FABRICATION AND MEASUREMENT OF A DUAL-POLARIZED APERTURE-COUPLED MICROSTRIP ANTENNA.....	44
5.IMPEDANCE CALCULATION OF A MICROSTRIP LINE FED H-SHAPED SLOT	48
Singularity Extraction Problem	56
5.1 Numerical Results.....	57
5.1.1 Mutual Impedance Calculation.....	58
5.2 Self Impedance Calculation of the Dipole.....	60
5.3 Results about Rectangular and H-shaped Slots	61
6.CONCLUSION.....	66
APPENDIX.....	68
Coefficient Calculation in x-direction	68
Triangle Convolution in x-direction	70
Step Function Convolution in y-direction.....	72
Integrals for Charge Functions.....	73
REFERENCES	76

LIST OF TABLES

TABLES

Table 1. 1 Different Types of Feeding Techniques of Microstrip Antennas	2
Table 3. 1 Parameters with Explanation used in a Design of an Aperture-Coupled Microstrip Antenna with a Single Rectangular Slot.	16
Table 3. 2 Parameters with Explanation used in a Design of an Aperture-Coupled Microstrip Antenna with a Single H-Shaped Slot.....	29
Table 3. 3 Parameters of a Designed Aperture-Coupled Microstrip Antenna with a Single H-Shaped Slot.....	37
Table 3. 4 Parameters of a Designed Aperture-Coupled Microstrip Antenna with Two Orthogonally Placed H-Shaped Slots.	42

LIST OF FIGURES

FIGURES

Figure 2. 1 Aperture-Coupled Microstrip Antenna with Parameters [19].	8
Figure 2. 2 Circuit Model for Aperture-Coupled Microstrip Antenna.	9
Figure 3. 1 General View of an Aperture-Coupled Microstrip Patch Antenna with a Rectangular Slot.	14
Figure 3. 2 Structure of a Designed Aperture-Coupled Microstrip Patch Antenna with a Rectangular Slot.	15
Figure 3. 3 Parameters used at the Design of an Aperture-Coupled Microstrip Antenna with a Single Rectangular Slot [29].	16
Figure 3. 4 Return Loss Parametric Analysis about Patch Length of an Aperture-Coupled Microstrip Antenna with a Single Rectangular Slot.	17
Figure 3. 5 Smith Chart of a Parametric Analysis about Patch Length of an Aperture-Coupled Microstrip Antenna with a Single Rectangular Slot.	17
Figure 3. 6 Return Loss Parametric Analysis about the Length of the Slot on the Aperture of an Aperture-Coupled Microstrip Antenna with a Single Rectangular Slot.	18
Figure 3. 7 Smith Chart of a Parametric Analysis about the Length of the Slot on the Aperture of an Aperture-Coupled Microstrip Antenna with a Single Rectangular Slot.	19
Figure 3. 8 Return Loss Parametric Analysis about the Width of the Slot on the Aperture of an Aperture-Coupled Microstrip Antenna with a Single Rectangular Slot.	20
Figure 3. 9 Smith Chart of a Parametric Analysis about the Width of the Slot on the Aperture of an Aperture-Coupled Microstrip Antenna with a Single Rectangular Slot.	20

Figure 3. 10 Return Loss Parametric Analysis about the Thickness of the Patch Substrate of an Aperture-Coupled Microstrip Antenna with a Single Rectangular Slot	21
Figure 3. 11 Smith Chart of a Parametric Analysis about the Thickness of the Patch Substrate of an Aperture-Coupled Microstrip Antenna with a Single Rectangular Slot	22
Figure 3. 12 Return Loss Parametric Analysis about the Length of the Stub of an Aperture-Coupled Microstrip Antenna with a Single Rectangular Slot.	23
Figure 3. 13 Smith Chart of a Parametric Analysis about the Length of the Stub of an Aperture-Coupled Microstrip Antenna with a Single Rectangular Slot.	23
Figure 3. 14 Return Loss Parametric Analysis about the Movement of the Slot in x-direction of an Aperture-Coupled Microstrip Antenna with a Single Rectangular Slot	24
Figure 3. 15 Smith Chart of a Parametric Analysis about the Movement of the slot in x-direction of an Aperture-Coupled Microstrip Antenna with a Single Rectangular Slot	25
Figure 3. 16 Return Loss Parametric Analysis about the Movement of the Slot in y-direction of an Aperture-Coupled Microstrip Antenna with a Single Rectangular Slot	26
Figure 3. 17 Smith Chart of a Parametric Analysis about the Movement of the slot in y-direction of an Aperture-Coupled Microstrip Antenna with a Single Rectangular Slot	26
Figure 3. 18 Return Loss Analysis for a Designed Aperture-Coupled Microstrip Antenna with a Single Rectangular Slot	27
Figure 3. 19 General View of an Aperture-Coupled Microstrip Patch Antenna with a Single H-Shaped Slot.....	28
Figure 3. 20 Parameters used at the Design of an Aperture-Coupled Microstrip Antenna with a Single H-Shaped Slot.	29
Figure 3. 21 Return Loss Parametric Analysis about the Length of the Stub of an Aperture-Coupled Microstrip Antenna with a Single H-Shaped Slot.	30

Figure 3. 22 Smith Chart of a Parametric Analysis about the Length of the Stub of an Aperture-Coupled Microstrip Antenna with a Single H-Shaped Slot.....	31
Figure 3. 23 Return Loss Parametric Analysis about the Length of the Center Slot of an Aperture-Coupled Microstrip Antenna with a Single H-Shaped Slot.....	32
Figure 3. 24 Smith Chart of a Parametric Analysis about the Length of the Center Slot of an Aperture-Coupled Microstrip Antenna with a Single H-Shaped Slot.....	32
Figure 3. 25 Return Loss Parametric Analysis about the Width of the Center Slot of an Aperture-Coupled Microstrip Antenna with a Single H-Shaped Slot.....	33
Figure 3. 26 Smith Chart of a Parametric Analysis about the Width of the Center Slot of an Aperture-Coupled Microstrip Antenna with a Single H-Shaped Slot.....	33
Figure 3. 27 Return Loss Parametric Analysis about the Length of the Slot Edge of an Aperture-Coupled Microstrip Antenna with a Single H-Shaped Slot.....	34
Figure 3. 28 Smith Chart of a Parametric Analysis about the Length of the Slot Edge of an Aperture-Coupled Microstrip Antenna with a Single H-Shaped Slot.	35
Figure 3. 29 Return Loss Parametric Analysis about the Width of the Slot Edge of an Aperture-Coupled Microstrip Antenna with a Single H-Shaped Slot.....	36
Figure 3. 30 Smith Chart of a Parametric Analysis about the Width of the Slot Edge of an Aperture-Coupled Microstrip Antenna with a Single H-Shaped Slot.	36
Figure 3. 31 Return Loss Analysis for a Designed Aperture-Coupled Microstrip Antenna with a Single H-Shaped Slot.	38
Figure 3. 32 Lengths and Widths of Two H-Shaped Slots.	39
Figure 3. 33 Return Loss Analysis for Two H-Shaped Slots.....	39
Figure 3. 34 General View of an Aperture-Coupled Microstrip Patch Antenna with Two Orthogonally Placed H-Shaped Slots.	40
Figure 3. 35 Parameters used at the Design of an Aperture-Coupled Microstrip Antenna with Two Orthogonally Placed H-Shaped Slots.....	41
Figure 3. 36 Return Loss Graph of Port 1 for a Designed Dual-Polarized Aperture-Coupled Microstrip Antenna with H-Shaped Slots.	42
Figure 3. 37 Return Loss Graph of Port 2 for a Designed Dual-Polarized Aperture-Coupled Microstrip Antenna with H-Shaped Slots.	43

Figure 3. 38 Isolation between Ports for a Designed Dual-Polarized Aperture-Coupled Microstrip Antenna with H-Shaped Slots.	43
Figure 4. 1 Parts and Total Structure of the Dual-Polarized Aperture-Coupled Microstrip Antenna with a Single Patch.	44
Figure 4. 2 Return Loss Comparisons between Fabricated and Simulated Dual-Polarized Aperture-Coupled Microstrip Antennas with a Single Patch for Port 1 and Port 2.....	45
Figure 4. 3 Fabricated Microstrip Feed Line and Microstrip Antenna with Open-Circuited Stubs.....	45
Figure 4. 4 Return Loss Comparison between Fabricated and Simulated Antennas with and without stubs for Port 1 and Port 2.	46
Figure 4. 5 Far Field Pattern Measurement Set-up.	46
Figure 4. 6 Far Field Pattern Comparisons between Simulation and Measurement at both Ports.	47
Figure 5. 1 Geometry of Slot fed by a Microstripline [30].....	48
Figure 5. 2 Sinusoidal Current Distribution on the Slot with Meshes.....	57
Figure 5. 3 Calculation of the Mutual Coupling Between Two Dipoles.	58
Figure 5. 4 Comparisons of the Mutual Impedance Characteristics of Two Dipoles with a Variation of the Distance Between Slots.	59
Figure 5. 5 Calculation of the Self Impedance of the Dipole.	60
Figure 5. 6 Comparison of the Self Impedance of the Dipole.	61
Figure 5. 7 Impedance Comparison of a Slot in the Ground Plane of a Microstripline (a) Results from [30], solid line:theory, x: measurement (b) Result from Equations above.	62
Figure 5. 8 Electric Fields for Rectangular and H-shaped Slots.....	63
Figure 5. 9 Meshing the H-shaped slot.....	64
Figure 5. 10 Modeling and Simulation Comparison for an H-Shaped Slot.....	64
Figure A. 1 Half Triangle Equations of Test and Base Triangles.....	68
Figure A. 2 Situations for the Convolution of Test and Base Half Triangles (a) left-left case,	69

Figure A. 3 Cases for the Convolution of Test and Base Triangles for all Situations.	70
Figure A. 4 Cases for the Convolution of Test and Base Functions in y-direction for all Situations.....	73
Figure A. 5 Cases for the Convolution of the Derivatives of Test and Base Functions for all Situations.....	74

CHAPTER 1

INTRODUCTION

In some applications like spacecraft, missile, aircraft and space applications, where performance, size, weight and cost are constraints, low-profile antennas are required. In order to respond these necessities, microstrip antennas can be considered as an attractive alternative. At the basic concept of microstrip antenna, it is composed of a radiating patch and a ground plane. These two elements are placed on different sides of a dielectric substrate.

In recent years, usage areas of microstrip antennas are increased due to their numerous advantages. Firstly, the most important advantage of microstrip antenna is its size and cost. At the production stage of microstrip antennas, small numbers of materials are used. These materials are the dielectric substrates and connectors. Therefore, microstrip antennas are light weight antennas and the production of the antennas are not costly. In addition, dielectric materials are thin and flexible, so microstrip antennas are low profile, low volume and conformal to any surfaces [2].

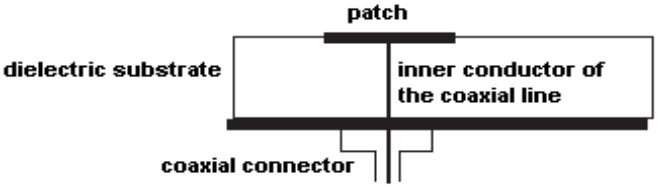
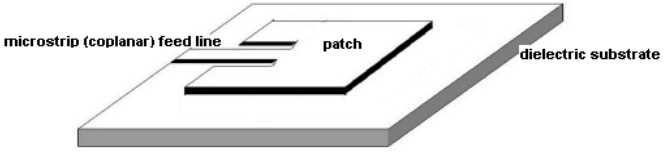
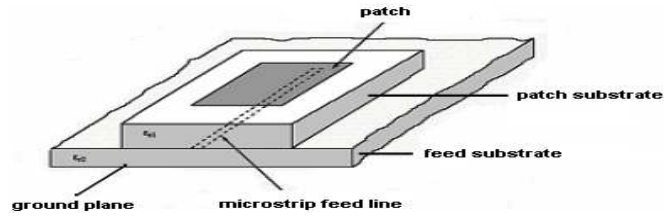
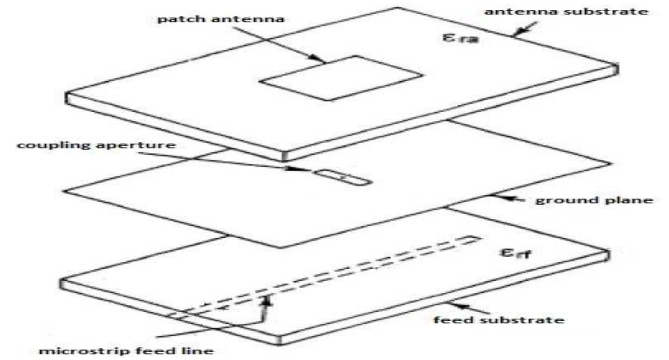
Secondly, radiation mechanisms of microstrip antennas are adjustable. This means that, it is easy to change the polarization of the microstrip antenna by changing the feed configuration. Therefore, the antenna can be easily made linearly or circularly polarized. Besides, in microstrip antennas, it is simple to make dual-polarization and dual-frequency operation [4].

Microstrip antennas are produced with printed circuit board infrastructure, so it is easy to integrate these antennas with microwave integrated circuits. Furthermore, the other advantage of printed circuit board production is that the production of

these antennas is fast because microstrip patch, feed lines and matching networks can be produced at the same time [1].

Along with the advantages of microstrip antennas, there are many disadvantages. The most important disadvantages of microstrip antennas are narrow bandwidth operation, low gain and low power handling capability. The bandwidth of a microstrip antenna can be increased by using an appropriate feeding method. Different types of feeding techniques that are most commonly used to excite microstrip antennas are listed in Table 1.1.

Table 1. 1 Different Types of Feeding Techniques of Microstrip Antennas

Feeding Technique	Image
Probe (Coaxial) feed	
Microstrip line feed	
Proximity (Electromagnetically) coupled feed	
Aperture-Coupled feed	

Coaxial feeds are the basic way of transferring power from the feed line to the patch by using a probe. At this feeding technique, the inner conductor of a connector passes through the dielectric substrate and then it is soldered to the microstrip patch and the outer conductor of the coaxial connector is soldered to the ground plane, as seen in Table 1.1 [13]. The most important parameter at the design of coaxial feeds is the selection of the location of the probe because impedance matching is provided by this parameter.

If the various feed configurations are compared in terms of manufacturing difficulty, it can be observed that the microstrip line feed configuration is the simplest one, because the feed and the patch are produced on the same substrate and the feed can be seen as an extended part of the patch, as seen in Table 1.1 [14]. Like a probe fed antenna, the feed location can be moved towards the center of the patch by using insets at either side of the feed line as shown in Table 1.1.

Proximity (electromagnetically) coupled feeds consist of two dielectric substrates. Patch lies on the upper substrate, microstrip feed line lies between the two substrates and the ground plane lies at the bottom of the lower substrate, as seen in Table 1.1 [16]. When the feed line is terminated at its open end, power couples to the patch by passing through the upper substrate. Therefore, another name given to this type of feed configuration is “electromagnetically coupled feed” [15]. The main advantage of this feed configuration is that wider bandwidth can be achieved with this configuration. Because, the dielectric constant and the thickness of the dielectric substrates for the feed line and the patch antenna can be chosen independently. Moreover, these parameters can be selected properly to widen the bandwidth of the antenna. As it is well known, a thin dielectric substrate with high dielectric constant should be chosen for the feed so that the fields will be confined under the feed line and spurious radiation from the feed line will be avoided. On the other hand, a thick dielectric substrate with low dielectric constant should be preferred for the patch antenna to obtain wider bandwidth. The reason is that, if the structure formed by the patch and the ground plane is considered as a capacitor, when the thickness of the substrate increases, the stored energy decreases, so the quality factor of the antenna decreases. As a result, the impedance bandwidth of the antenna increases. Similarly,

when the dielectric constant of the substrate decreases, the stored energy also decreases, but the radiated power increases due to the larger fringing fields and consequently the quality factor decreases. Therefore, the impedance bandwidth of the antenna increases.

Aperture coupled microstrip feeds are used in large bandwidth required applications. This feed structure includes also two dielectric substrates. Microstrip patch is located on the upper substrate, antenna substrate, microstrip line is located on the lower substrate, feed substrate, and ground plane is located between these two substrates. Besides, coupling slot is located in the ground plane as seen in Table 1.1 [19]. At this type of feed configuration, coupling is provided from the microstrip feed line to the microstrip patch through the slot. Bandwidth is enhanced by various parameters for this configuration. These are slot parameters and dielectric substrates parameters as discussed for the electromagnetically coupled feeds. In addition, in aperture-coupled configuration, there exist two resonances, namely slot and patch. Therefore, bandwidth can be enhanced by letting these resonances to be close to each other. The radiation of this type of feed structure is better than the other types mentioned above because the radiation from the open ended microstrip feed line does not affect the radiation pattern of the antenna due to the ground plane. This property improves the polarization purity. Furthermore, the backlobe radiation is almost 15-20dB below the forward beam radiation at this type. However, the back radiation from the slot may need to be decreased by locating a metal plane at some distance from the bottom part of the feed substrate. At the design process, in order to increase bandwidth, the slot should be located at the center of the microstrip patch. This increases the coupling between the magnetic field of the patch and the magnetic current on the slot [2]. By using bandwidth enhancement techniques described above, nearly 20% bandwidth is achieved.

The main aim of this thesis is to design a wideband dual-polarized microstrip antenna operating at X-band. Dual polarization operation makes the antenna transmit twice as much data compared with a single polarized antenna. To satisfy the requirement on the bandwidth of the antenna, aperture coupled feed structure is chosen. Dual polarization capability can be obtained by placing two orthogonal

feeds. This was first demonstrated by Adrian and Schaubert. Two orthogonal feeds with two orthogonal coupling apertures on the ground plane were used to feed a single square microstrip patch. Dual linear polarization can be obtained with this structure with 18dB isolation between the feed lines [9]. The main problem at this approach is the asymmetry and the size of the coupling slots on the ground plane. The coupling level decreases because at some designs, orthogonal slots can not be fit into the area of the patch. In addition to this, these structures limit the isolation and polarization purity. For the requirement of wideband dual-polarized aperture-coupled microstrip antennas, two orthogonally placed H-shaped slots can be used, but the cross polarization is high at this type of placement. In order to avoid this drawback, the end of the H-slots can be bended and better isolation levels can be achieved [12]. Another approach to increase the isolation was suggested by Tsao, Hwang, Killburg and Dietrich. In this approach, crossed slots were used and it was observed that this application increases the isolation, 27dB, without decreasing the bandwidth of the aperture-coupled microstrip antenna. However, it was seemed that it is difficult to feed each arm of the crossed slot since crossover in the balanced feed lines is required. Another approach for feeding the crossed slot for dual polarization is achieved by placing orthogonal feed lines on different dielectric substrates [7].

In a previous study it is reported that [20], 10% bandwidth requirement can be satisfied at 1GHz through the use of H-shaped slots for dual-polarization operation. In this thesis, resonant frequency is adjusted at 9.5GHz and the bandwidth of the antenna is aimed to be 20%. Same as [20], dual polarization operation is tried to be supplied.

Initially, slot coupled microstrip antenna with a rectangular aperture is investigated and the effects of various parameters on the bandwidth performance of the antenna are studied. Then, slot coupled microstrip antenna with an H-shaped aperture is studied in a similar way and an antenna with 20% bandwidth is designed. All the analyses are done on CST Microwave Studio®.

After that, it is focused on the dual polarization operation with two orthogonally placed H-shaped slots. The same bandwidth requirement and return loss characteristics are tried to be supplied for both ports.

At the final part, the dual-polarized antenna is manufactured and the simulation and the measurement results are compared.

During the analysis at the design step, it is realized that bandwidth of an H-shaped slot is wider than the rectangular slot. In order to investigate the reason of this observation, the variation of the input impedance of a microstrip line fed H-shaped slot with respect to frequency is analyzed by using the approach proposed by Pozar [30] which is based on the reciprocity theorem. In this approach the slot is modeled as a series impedance in the microstrip feed line. This method was first proposed to analyze rectangular slots, in this thesis it is extended for the analysis of H-shaped slots. Furthermore, in Pozar's approach, the spectral domain Green's functions are used to model the effects of dielectric slab. In this thesis, spatial domain approach is preferred and the spatial domain Green's functions are approximated by using Discrete Complex Image Method (DCIM) [35]. A MATLAB code is developed to calculate the impedance of microstrip line fed H-shaped slot.

This thesis is organized in five chapters as follows:

Chapter 2 gives some information about aperture-coupled microstrip antennas and properties of these types of antennas. In addition, effects of the parameters on the antenna performance are discussed.

Chapter 3 includes the analysis of an aperture-coupled microstrip antenna with rectangular shaped slots and H-shaped slots. In addition to that, dual-polarization operation is investigated for both slot shapes. After all the analysis, a wideband and dual-polarized aperture-coupled microstrip antenna is designed with H-shaped slots. The designed dual-polarized aperture-coupled microstrip antenna is fabricated. After fabrication process is completed, antenna input return loss and radiation pattern are measured. The measurement results and their comparison with simulation results are presented in Chapter 4.

Chapter 5 includes the reciprocity theorem based formulation for the calculation of the impedance of a microstrip line fed slot aperture. The comparisons of simulation results for rectangular and H-shaped slots are also presented in this chapter.

Finally, a conclusion is provided in Chapter 6.

CHAPTER 2

APERTURE- COUPLED MICROSTRIP ANTENNAS

Aperture-coupled microstrip antennas consist of two dielectric substrates. The microstrip patch is printed on the upper substrate. The coupling aperture is located between upper and lower substrates and the microstrip feed line is printed on the bottom part of the lower substrate, Figure 2.1. The microstrip patch is coupled through an aperture or slot in the common ground plane by a microstrip feed line. Coupling occurs at the dominant mode of the microstrip patch because the slot interrupts the longitudinal current flow in them [1].

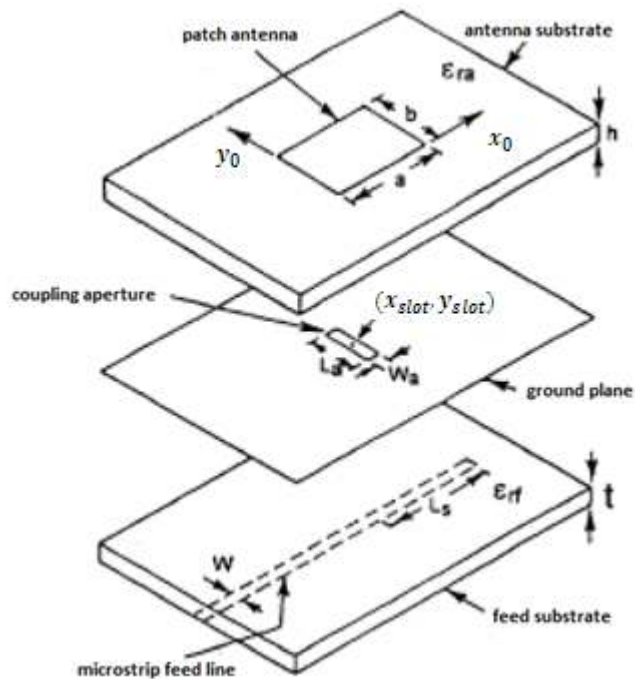


Figure 2. 1 Aperture-Coupled Microstrip Antenna with Parameters [19].

In literature, various equivalent circuit networks are proposed to model aperture coupled microstrip antennas [36, 37]. Although these different networks possess some slight variations from each other, the circuit model shown in Figure 2.2 is found to be the network which gathers most of the common characteristics of the proposed models. In this network the transformer with 1:n turn ratio models the coupling between the feed line and the antenna, Y_s and Y_a represent the admittance of the slot and the patch, respectively. The calculation of the turn ratio, n , and the slot admittance, Y_s , by using reciprocity theorem will be presented in Chapter 5. Here this equivalent circuit model is presented to support the discussions about the effects of antenna parameters on the input impedance characteristics of the antenna.

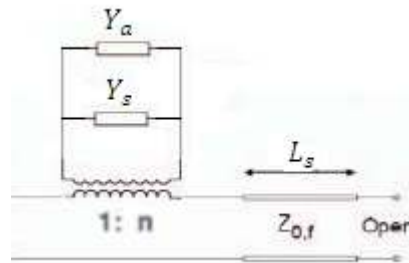


Figure 2. 2 Circuit Model for Aperture-Coupled Microstrip Antenna.

During the design process of aperture-coupled microstrip antennas, many parameters should be investigated. These parameters, shown in Figure 2.1, are the dimensions of printed metal materials and the selection of dielectric substrates. The effects of these parameters on the input impedance characteristics of aperture-coupled microstrip antennas are summarized below:

Feed Substrate Dielectric Constant (ϵ_{rf}):

This parameter has an effect on the coupling from the microstrip feed line to the slot. For good microstrip qualities, the dielectric constant of a feed substrate is chosen in the range 2 to 10.

Feed Substrate Thickness (t):

This parameter has an effect on spurious radiation from the microstrip feed line. For less spurious radiation, the feed substrate thickness should be chosen low, in the range of 0.01λ to 0.02λ .

Feed Line Width (W):

This parameter has an effect on the characteristic impedance of the microstrip feed line.

Slot Length (L_a):

This parameter has an effect on the resonance frequency of the antenna and the coupling level between the microstrip feed line and the microstrip patch. Also, if the slot length increases, the resonant resistance of the antenna increases. Therefore, it should be adjusted well for good impedance matching. In addition, slot length determines the back radiation level of the microstrip antenna because when the coupling exists from the feed line to the aperture, the slot radiates in both directions (upper and lower half spaces).

Slot Width (W_a):

This parameter has an effect on the coupling level between the microstrip feed line and the microstrip patch, but this effect is not as much as the effect of the slot length. The ratio of the slot width to the slot length should be nearly 1/10.

Antenna Substrate Dielectric Constant (ϵ_{ra}):

This parameter has an effect on the radiation efficiency and bandwidth of the microstrip antenna. In order to increase the bandwidth of the antenna, the dielectric constant of the antenna substrate should be chosen as low. Besides, the surface wave excitation can be decreased by choosing substrates with lower dielectric constants.

Antenna Substrate Thickness (h):

This parameter has an effect on the coupling level between the aperture and the microstrip patch and bandwidth of the microstrip antenna. When the thickness of the substrate increases, the coupling level decreases; however, the bandwidth of the antenna increases. In addition, this parameter also affects the resonant resistance of the antenna. The resonant resistance decreases by increasing the thickness of the substrate. Therefore, this parameter should be adjusted by considering these effects.

Microstrip Patch Length (b):

This parameter has an effect on the resonant frequency of the microstrip antenna. The resonant frequency decreases by increasing the length of the microstrip patch.

Microstrip Patch Width (a):

This parameter has an effect on the resonant resistance of the microstrip antenna. The resonant resistance decreases by increasing the width of the microstrip patch. Besides, when the length and the width of the patch are chosen to be equal, i.e. square patch configuration, the level of the cross polarization increases. Therefore, if the requirement of the antenna is not dual polarization or circular polarization, they should not be chosen as equal.

Position of Slot Relative to Microstrip Patch (x_0, y_0):

This parameter has an effect on the coupling level between the aperture and the microstrip patch. The slot should be placed at the center of the patch for maximum coupling. When the patch moves in the direction of H-plane over the slot, there is a small decrease at the coupling level. However, when the patch moves in the direction of E-plane, there is a huge decrease at the coupling level [26].

Length of Tuning Stub (L_s):

This parameter is used for tuning the excess reactance of the microstrip antenna. The length of the stub is typically slightly less than $\lambda_g/4$, where λ_g is the guided wavelength [7]. This parameter is used for matching the antenna successfully. If the

length of the tuning stub decreases, the impedance locus on the Smith Chart moves in the capacitive direction.

In the next chapter some parametric analysis will be performed to investigate the effects of these parameters on the input impedance characteristics of the antenna.

CHAPTER 3

PARAMETRIC STUDY OF APERTURE- COUPLED MICROSTRIP ANTENNAS

3.1 Introduction

Aperture-coupled microstrip antenna with a single rectangular slot, aperture-coupled microstrip antenna with a single H-shaped slot and aperture-coupled microstrip antenna with two orthogonal H-shaped slots are analyzed in this chapter. All the analyses are done in CST Microwave Studio 2010® commercial software.

In the first part, effects of parameters on aperture-coupled microstrip antenna with a single rectangular slot are observed. The required bandwidth of the antenna is tried to be achieved with a rectangular slot and the possibility of designing this antenna with two orthogonal rectangular slots are examined. All the analyses are done at X-band (8-12 GHz) and the center frequency of the design is adjusted as 9.5 GHz.

In the second part, effects of parameters on aperture-coupled microstrip antenna with a single H-shaped slot are observed. With an H-shaped slot, wideband characteristic with a smaller slot length is tried to be satisfied.

In the last part, effects of parameters on aperture-coupled microstrip antenna with two orthogonal H-shaped slots are observed. Wide bandwidth characteristics are tried to be obtained for two polarizations. Furthermore, mutual coupling between these two slots is investigated at this configuration.

3.2 Analysis at the Design of an Aperture-Coupled Microstrip Patch Antenna with a Single Rectangular Slot

At this section, parametrical analyses about aperture-coupled microstrip antenna with a single rectangular slot are given. Structure of the antenna is shown in Figure 3.1.

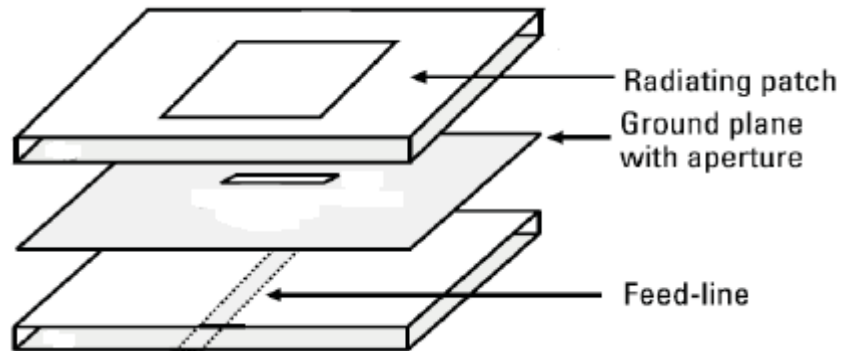


Figure 3. 1 General View of an Aperture-Coupled Microstrip Patch Antenna with a Rectangular Slot.

Two dielectric substrates are used at the design of the antenna. The upper dielectric layer is settled between the microstrip patch and the ground plane. The lower dielectric layer is settled between the ground plane and the microstrip feed line. In addition, microstrip patch is located on a dielectric material above the patch and this material is used as a radome for antenna. At the beginning of the design, dielectric substrates are selected in accordance with the dielectric constants and availabilities for the materials. Consequently, Rogers Corporations material RO4003 ($\epsilon_r = 3.55, h = 0.508mm$), at the feed and radome side, and ROHACELL foam ($\epsilon_r = 1.025$), at the patch side, are selected. The structure of the antenna is given in Figure 3.2.

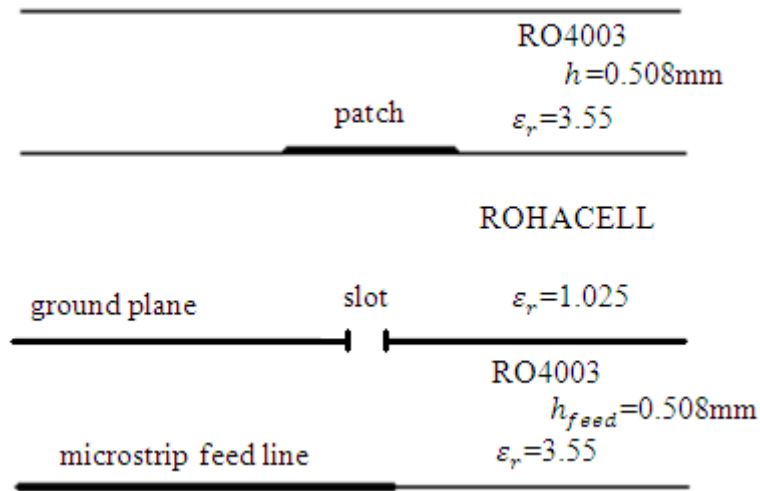


Figure 3. 2 Structure of a Designed Aperture-Coupled Microstrip Patch Antenna with a Rectangular Slot.

For this choice of dielectric substrate, the width of the feed line for 50Ω characteristic impedance is found to be 1.1 mm. Besides, length and width of dielectric substrates are chosen as 25 mm.

3.2.1 Parameters used in the Aperture-Coupled Microstrip Antenna Design with a Single Rectangular Slot

There exist many parameters at the design of an aperture-coupled microstrip antenna with a single rectangular slot. These parameters have an effect on the coupling level, the bandwidth, and the resonant resistance of the antenna. These parameters are shown in Figure 3.3 and their explanations are given in Table 3.1. During the parametric analysis, one of the parameters is varied within a range listed in Table 3.1 and all other parameters are kept constant at their nominal values which are also given in Table 3.1.

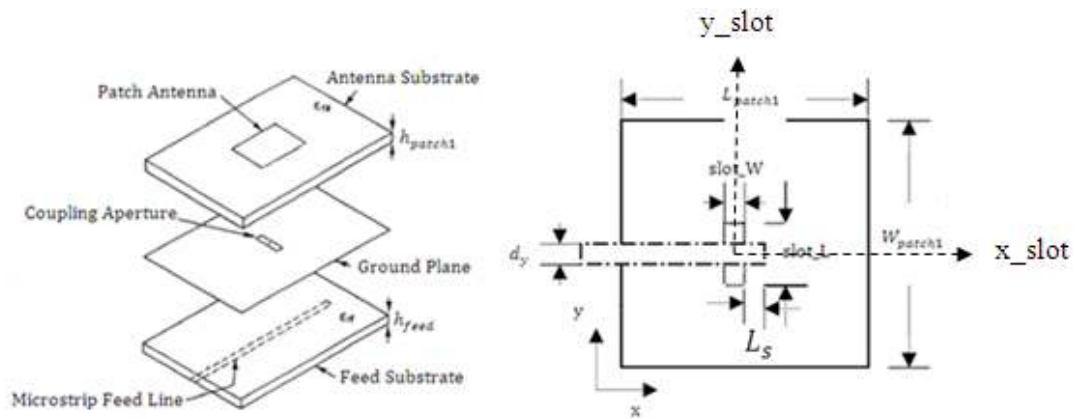


Figure 3. 3 Parameters used at the Design of an Aperture-Coupled Microstrip Antenna with a Single Rectangular Slot [29].

Table 3. 1 Parameters with Explanation used in a Design of an Aperture-Coupled Microstrip Antenna with a Single Rectangular Slot.

Name of the Parameter	Definition of the Parameter	Parameter Range	Nominal Value
L_{patch1}	Length of the Patch	8.9...10.9mm	9.9mm
W_{patch1}	Width of the Patch	8.9...10.9mm	9.9mm
L_s	Stub Length	1.3...2.5mm	1.9mm
h_{patch1}	Thickness of the Patch Substrate	1.5...3.5mm	2.5mm
slot_L	Length of the Slot	8.1...9.3mm	8.7mm
slot_W	Width of the Slot	0.4...0.8mm	0.6mm
x_{slot}	Slot Position Relative to the Patch in x-direction	-2...0mm	0mm
y_{slot}	Slot Position Relative to the Patch in y-direction	-2...0mm	0mm

3.2.2 The Parametrical Analysis on the Length of the Microstrip Patch

Effects of length of the microstrip patch on the resonant frequency are given in this section. Parametric analysis about the return loss and bandwidth characteristic of an antenna is done by changing the length of the patch from 8.9mm to 10.9mm as seen

in Figure 3.4. Additionally, results are also observed on the Smith Chart and presented in Figure 3.5.

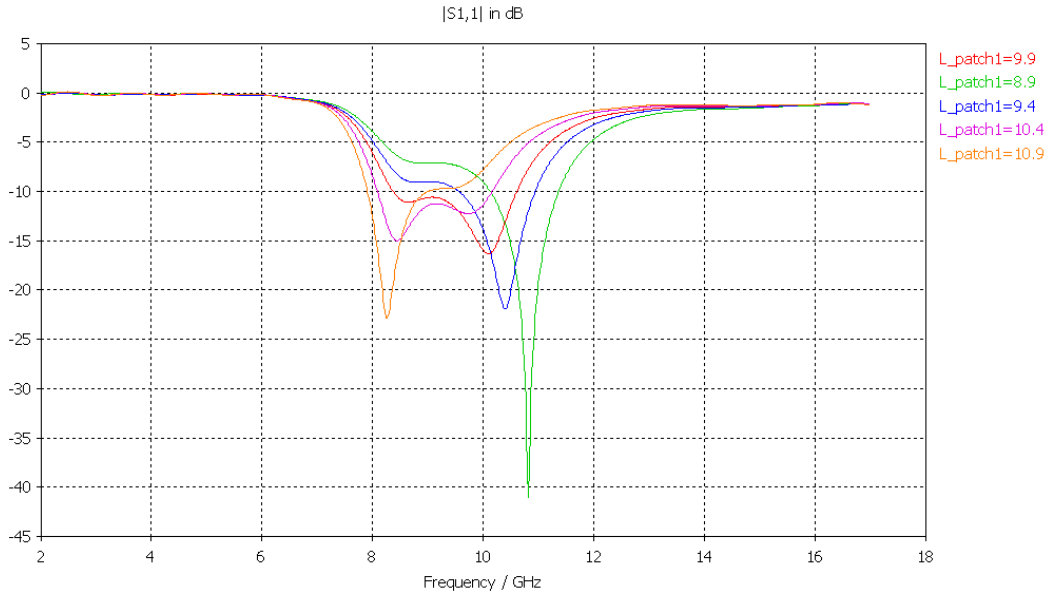


Figure 3. 4 Return Loss Parametric Analysis about Patch Length of an Aperture-Coupled Microstrip Antenna with a Single Rectangular Slot.

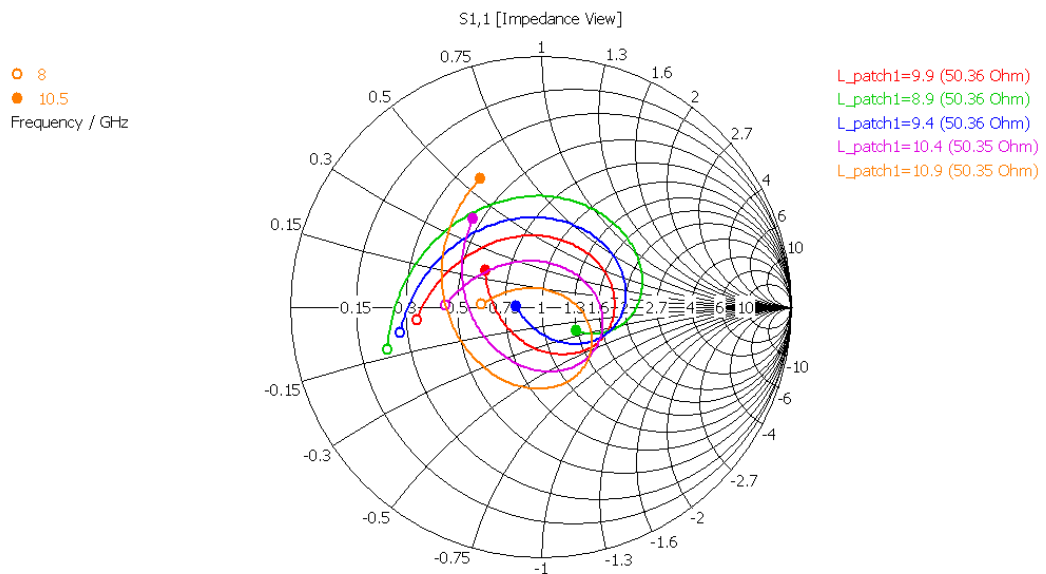


Figure 3. 5 Smith Chart of a Parametric Analysis about Patch Length of an Aperture-Coupled Microstrip Antenna with a Single Rectangular Slot.

It is seen from Figure 3.4 that, resonant frequency of an aperture-coupled microstrip antenna decreases when the length of the patch increases. In Figure 3.4, the lower

resonance shows the resonance of the microstrip patch. Moreover, from Figure 3.5, it can be observed that the impedance locus circle moves in capacitive direction when the length of the patch increases. For good matched design, the impedance locus circle should be at the center of the Smith Chart and it should fit in VSWR=2 circle. Therefore, length of the patch is selected by examining these results.

Width of the microstrip patch has also an effect on the characteristics of the microstrip antenna. However, goal of this thesis is to design a dual polarized antenna, so in all design cases, the width of the patch is chosen to be equal to the length of the patch, so that a square patch is considered.

3.2.3 The Parametrical Analysis on the Length of the Slot on the Aperture

This section includes the effects of the length of the slot on return loss and bandwidth characteristics of the microstrip antenna. Parametric analysis is done to investigate this effect. Analyses for return loss and bandwidth are done by changing the slot length values parametrically from 8.1mm to 9.3mm. Result of this analysis is given in Figure 3.6. In addition, parametric analysis effects on the input impedance are seen on the Smith Chart, Figure 3.7.

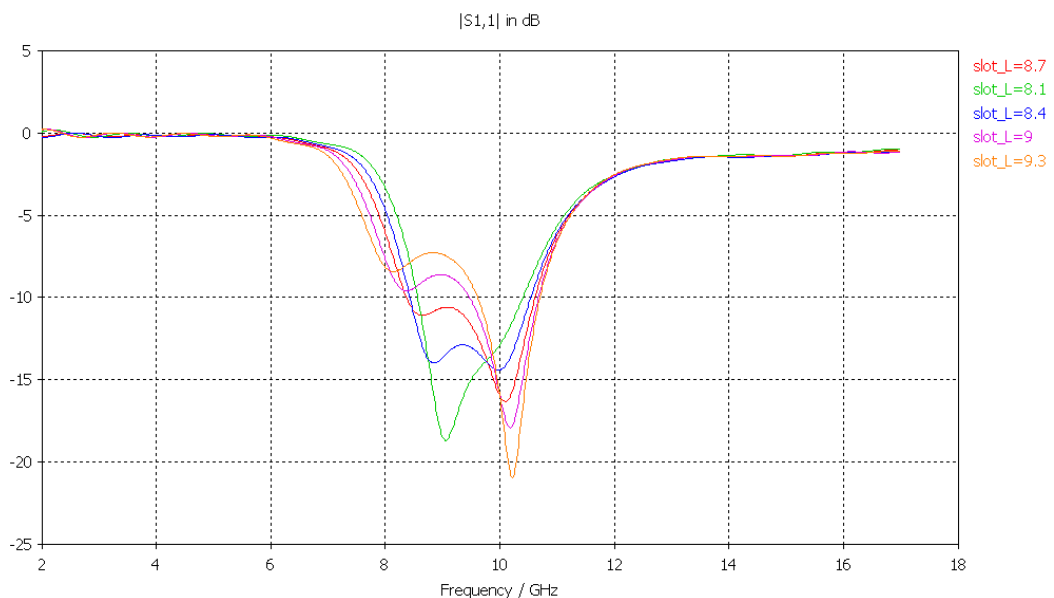


Figure 3. 6 Return Loss Parametric Analysis about the Length of the Slot on the Aperture of an Aperture-Coupled Microstrip Antenna with a Single Rectangular Slot.

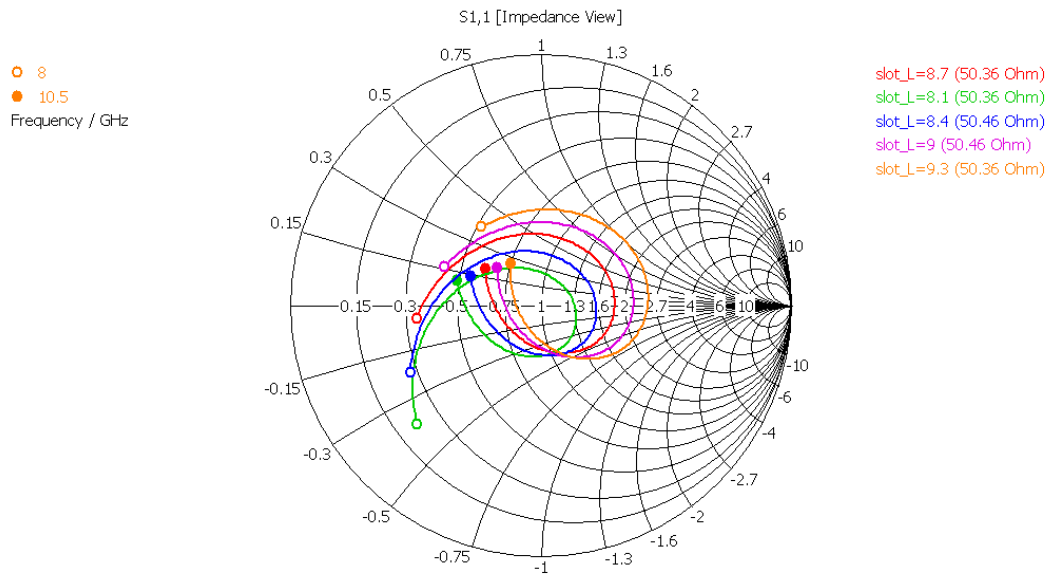


Figure 3. 7 Smith Chart of a Parametric Analysis about the Length of the Slot on the Aperture of an Aperture-Coupled Microstrip Antenna with a Single Rectangular Slot.

As seen from Figure 3.6, variation on the slot length has an effect on the coupling level of the antenna. If the length of the slot increases, level of return loss value becomes deeper and diameter of the circle on the Smith Chart, Figure 3.7, becomes larger.

3.2.4 The Parametrical Analysis on the Width of the Slot on the Aperture

Effects of the width of the slot on return loss and bandwidth characteristics are given in this section. Analyses are done parametrically in order to observe the effect on the characteristics. At the analysis, parameter value varies between 0.4mm and 0.8mm. Figure 3.8 shows the result of this analysis. Parametric analysis is also investigated to see the change on the input impedance by using Smith Chart, Figure 3.9.

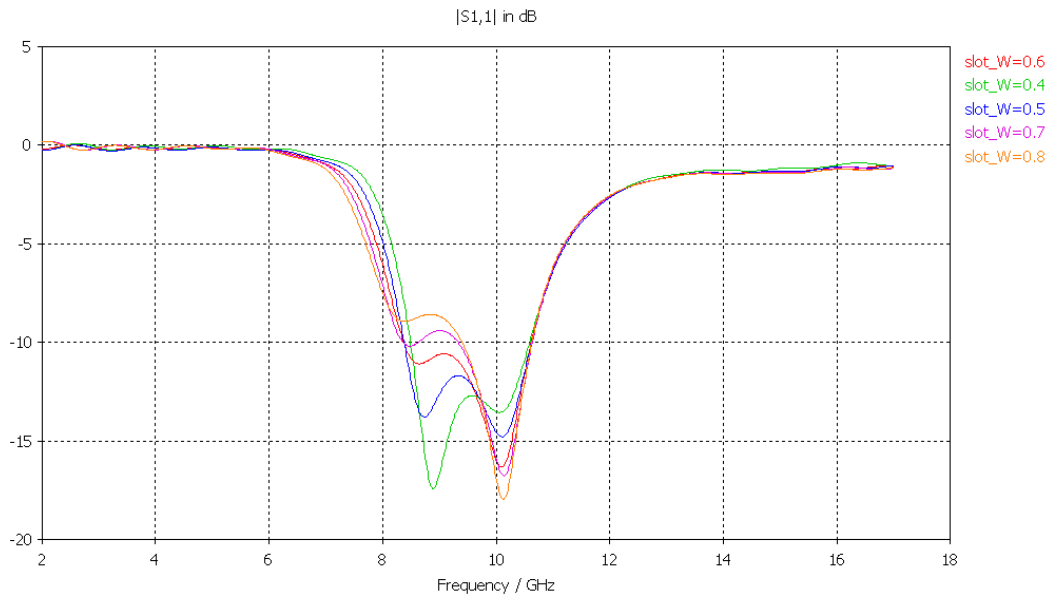


Figure 3. 8 Return Loss Parametric Analysis about the Width of the Slot on the Aperture of an Aperture-Coupled Microstrip Antenna with a Single Rectangular Slot.

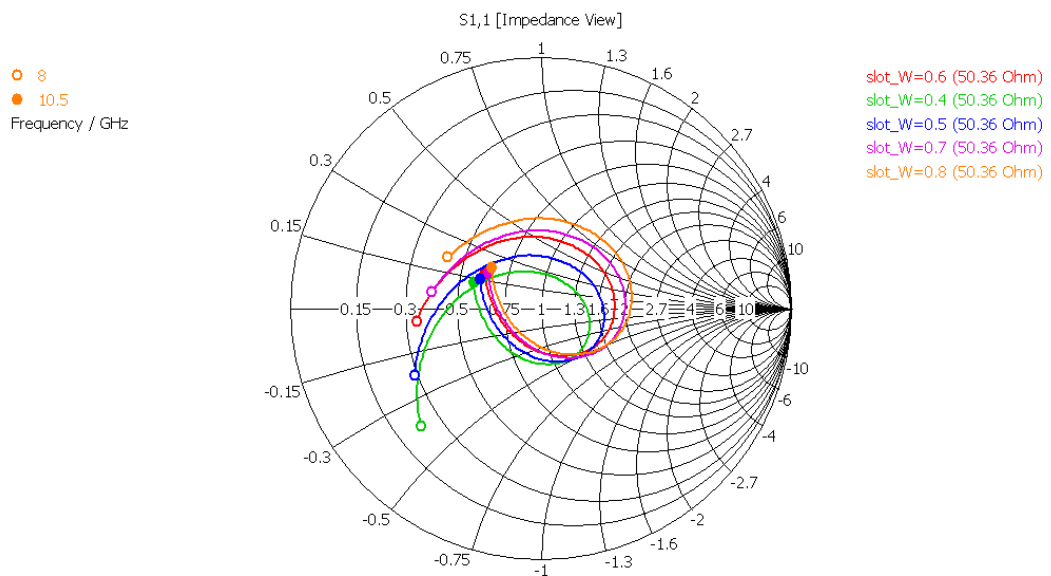


Figure 3. 9 Smith Chart of a Parametric Analysis about the Width of the Slot on the Aperture of an Aperture-Coupled Microstrip Antenna with a Single Rectangular Slot.

Variation of slot width has an effect on the coupling level of the antenna. However, this effect is smaller than the effect of the slot length. It can be seen from Figure 3.8 that, level of return loss value becomes deeper when the width of the slot increases.

Moreover, diameter on the circle of the Smith Chart increases when the width of the slot increases.

3.2.5 The Parametrical Analysis on the Thickness of the Patch Substrate

In this section, effects of the thickness of patch substrate on the bandwidth of the antenna are studied. Return loss and bandwidth analyses are done by changing the thickness values parametrically between 1.5mm and 3.5mm. Result of this analysis is given in Figure 3.10. In addition, results are observed on the Smith Chart and this makes the analysis more comprehensible, Figure 3.11.

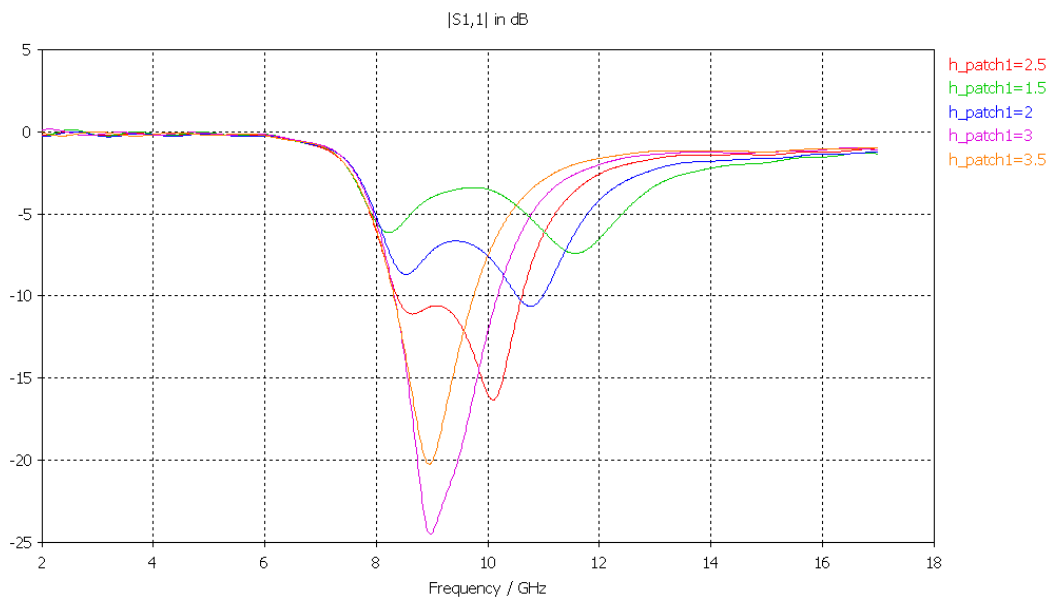


Figure 3. 10 Return Loss Parametric Analysis about the Thickness of the Patch Substrate of an Aperture-Coupled Microstrip Antenna with a Single Rectangular Slot.

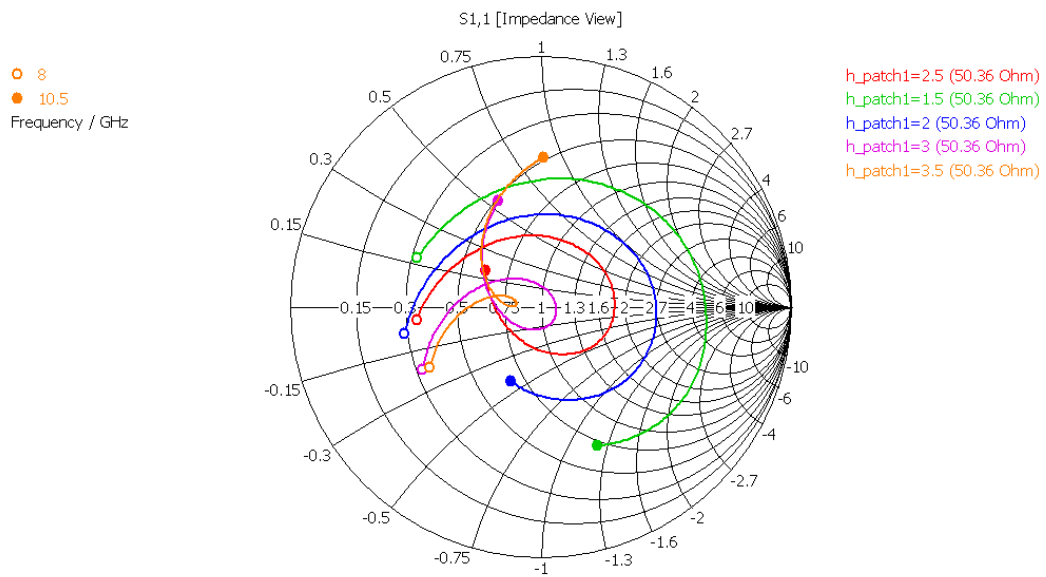


Figure 3. 11 Smith Chart of a Parametric Analysis about the Thickness of the Patch Substrate of an Aperture-Coupled Microstrip Antenna with a Single Rectangular Slot.

It is seen from Figure 3.10 that, thickness of the patch substrate has an important effect on the bandwidth characteristics of the antenna. The patch substrate has to be thick for wideband operation. However, when the thickness increases, coupling level decreases. In order to prevent this effect, length of the slot has to be increased. One of the resonances disappear, two resonances come closer, when thickness increases, Figure 3.10. Additionally, when the thickness increases, diameter of the circle on Smith Chart decreases, as seen from Figure 3.11.

3.2.6 The Parametrical Analysis on the Length of the Stub

Effects of the length of the stub on return loss and bandwidth characteristics of the antenna are given in this section. Analyses on the bandwidth and return loss are realized by changing the length value parametrically between 1.3mm and 2.5mm. Result of this analysis is shown in Figure 3.12 and the effect of the parametric analysis on the input impedance on Smith Chart is observed in Figure 3.13.

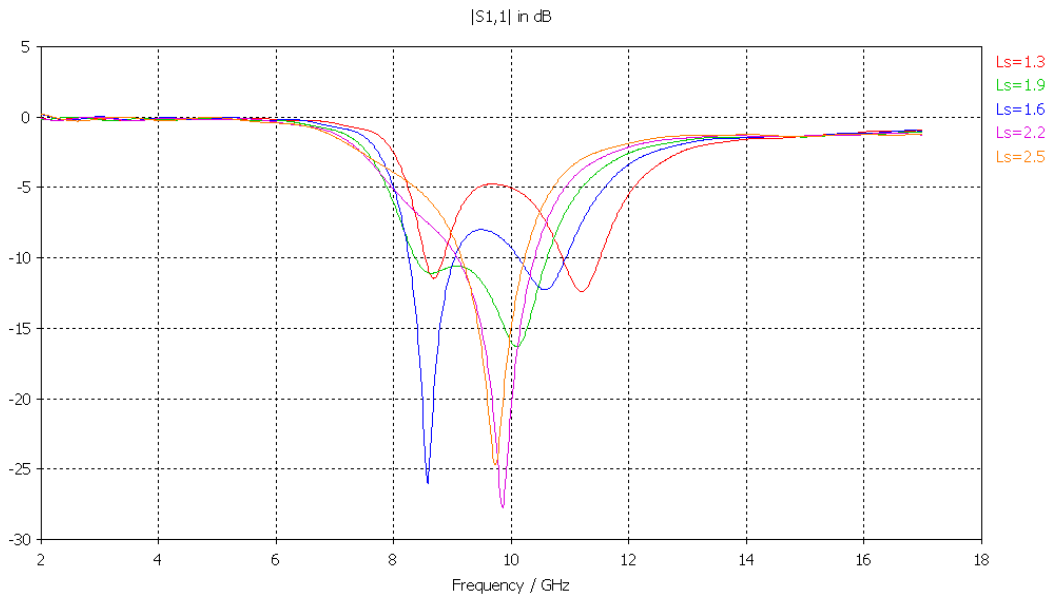


Figure 3.12 Return Loss Parametric Analysis about the Length of the Stub of an Aperture-Coupled Microstrip Antenna with a Single Rectangular Slot.

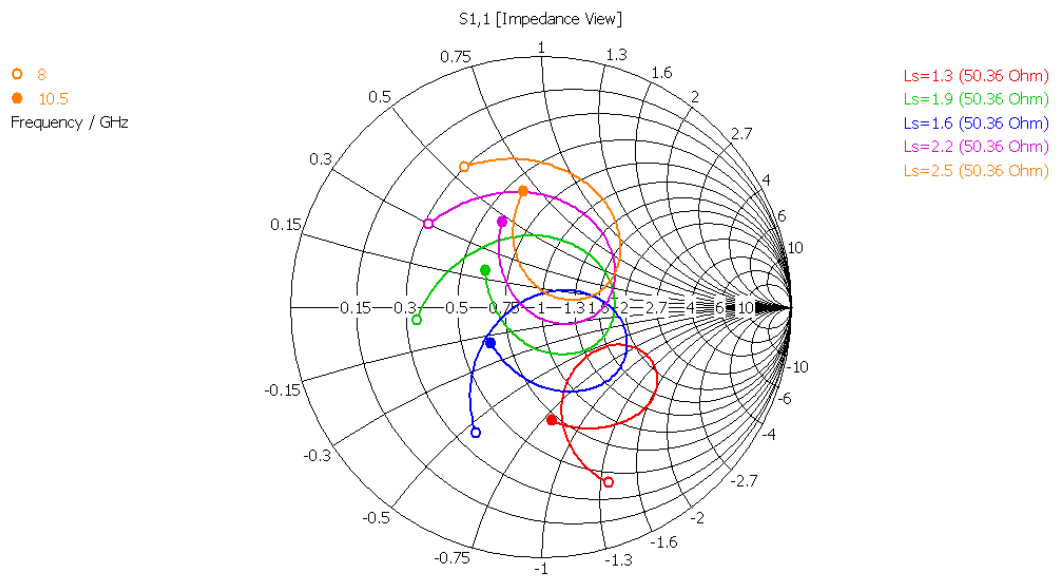


Figure 3.13 Smith Chart of a Parametric Analysis about the Length of the Stub of an Aperture-Coupled Microstrip Antenna with a Single Rectangular Slot.

Variation of the length of the tuning stub has an effect on adjusting the excess reactance of the microstrip antenna. This parameter is used for matching the antenna. As seen from Figure 3.12, for different values of stub length, there exists a significant change on return loss characteristics. In addition, Figure 3.13 shows that

when the length of the stub increases, Smith Chart circle moves in inductive direction.

3.2.7 The Parametrical Analysis regarding the Displacement of the Slot in x-Direction

In this section, effects of the movement of the slot in x-direction on return loss and bandwidth characteristics are investigated. Parametric analyses are done by moving the slot in x-direction from -2mm to 0mm. Results of this analysis are shown in Figure 3.14 and the Smith Chart including the results on the change of the input impedance is shown in Figure 3.15.

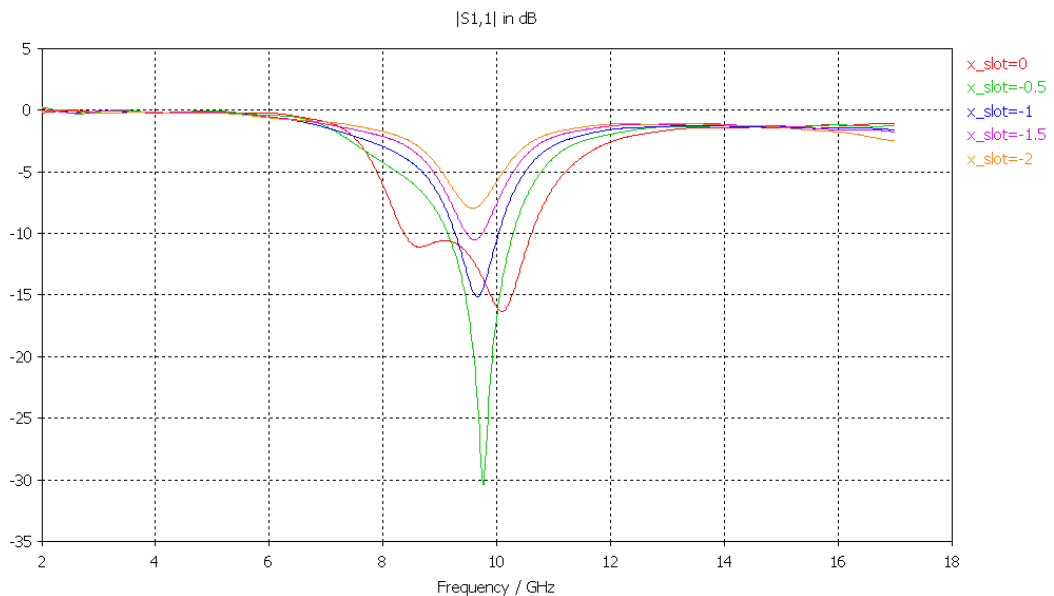


Figure 3. 14 Return Loss Parametric Analysis about the Movement of the Slot in x-direction of an Aperture-Coupled Microstrip Antenna with a Single Rectangular Slot.

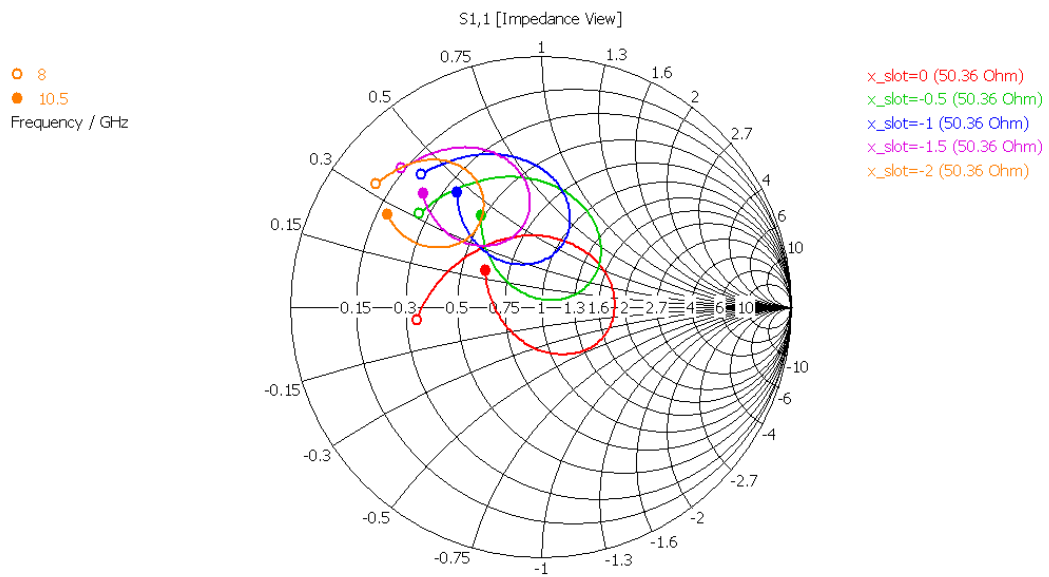


Figure 3. 15 Smith Chart of a Parametric Analysis about the Movement of the slot in x-direction of an Aperture-Coupled Microstrip Antenna with a Single Rectangular Slot.

Variation on the position of the slot relative to patch in x-direction has an effect on the coupling level of the antenna. When the slot is at the center of the patch, the impedance circle is closer to the center of the Smith Chart. As the offset increases, coupling level decreases and the input impedance circle moves away from the center of the Smith Chart.

3.2.8 The Parametrical Analysis regarding the Displacement of the Slot in y-Direction

This section includes the effects of the movement of the slot in y-direction on return loss and bandwidth characteristics. Parametrical analyses are done by moving the slot between -2mm to 0mm by taking the center of the patch as reference. Result of this analysis is given in Figure 3.16 and parametric analysis including the effects of the parameter variation on the input impedance at the Smith Chart is given in Figure 3.17.

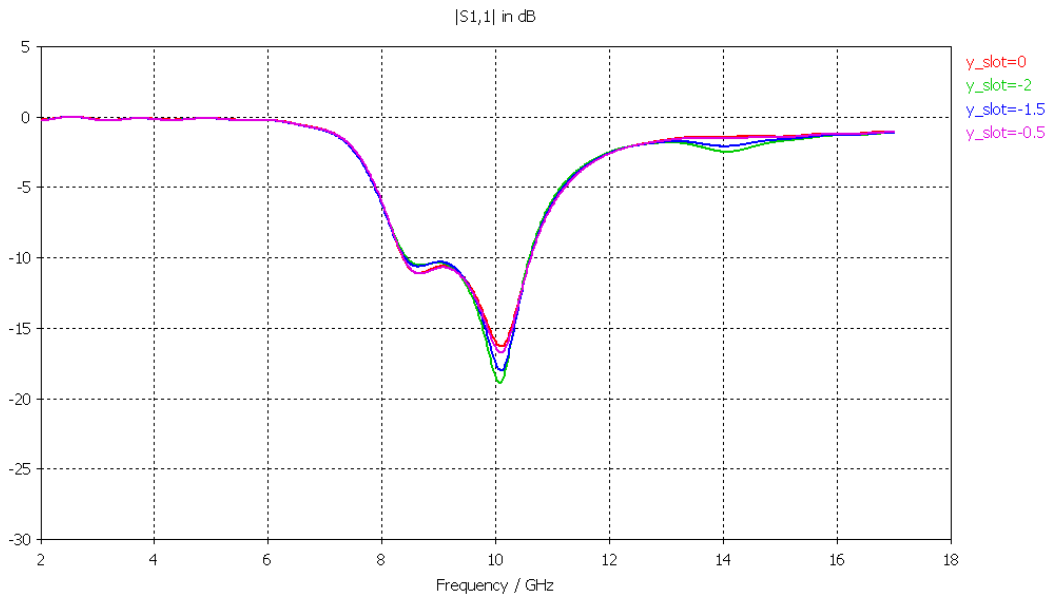


Figure 3.16 Return Loss Parametric Analysis about the Movement of the Slot in y-direction of an Aperture-Coupled Microstrip Antenna with a Single Rectangular Slot.

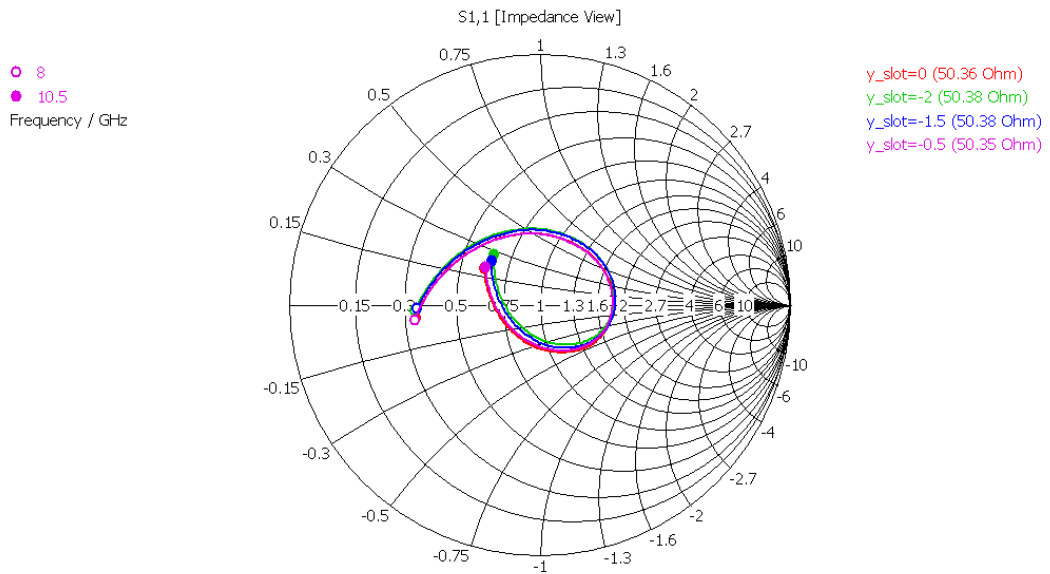


Figure 3.17 Smith Chart of a Parametric Analysis about the Movement of the slot in y-direction of an Aperture-Coupled Microstrip Antenna with a Single Rectangular Slot.

At the Figure 3.16 and 3.17, behaviors of the parameters are same for symmetric movement of the slot. Resonant frequency and coupling level is not affected by moving the slot relative to the patch in y-direction.

The reason for the variation on return loss and input impedance characteristics, regarding the displacement of the slot in x- and y-directions, is that the dominant mode excited in the microstrip antenna is TE_{10} mode. This mode exhibits a sinusoidal variation in x-direction and it is constant in y-direction. Consequently, the coupling between the slot and the patch becomes maximum when the offset in x-direction is zero, but variations in the position of the slot in y-direction do not have any significant effect.

Aim of this thesis is to design an antenna with a 20% bandwidth. After all these parameters are analyzed, the wideband antenna with a rectangular slot is designed. Return loss and bandwidth characteristic of this design is shown in Figure 3.18.

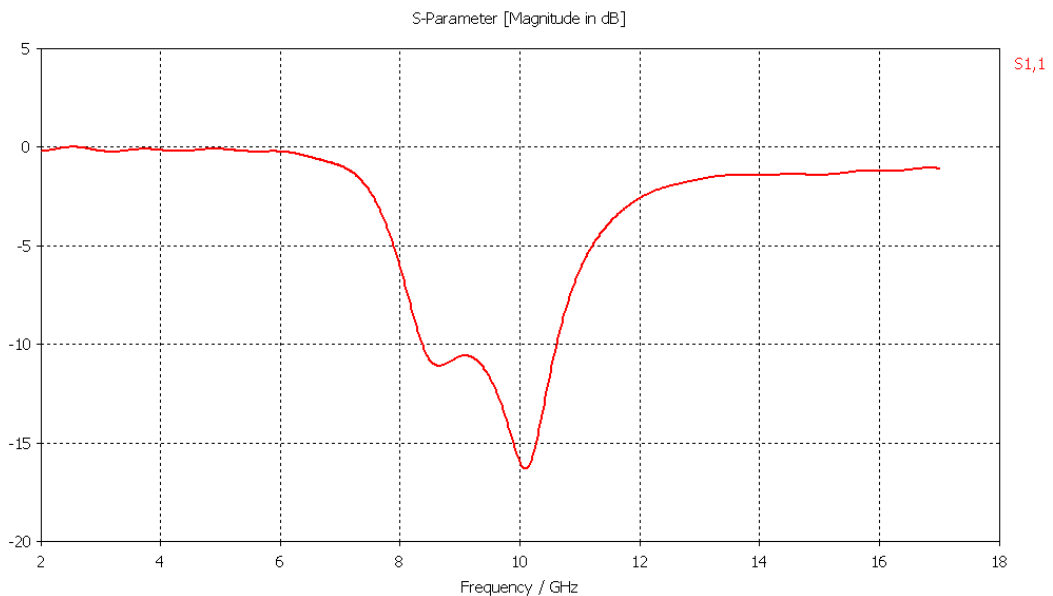


Figure 3. 18 Return Loss Analysis for a Designed Aperture-Coupled Microstrip Antenna with a Single Rectangular Slot.

As seen from Figure 3.18, 20% bandwidth requirement is provided with this design. Another necessity of this thesis is that antenna should be dual-polarized. However, length of the slot has to be long in rectangular slotted applications for wideband applications. It is seemed to be impossible to feed the patch with two orthogonally placed rectangular slots. Therefore, alternative design techniques are researched in order to solve this problem and the same bandwidth is tried to be handled with H-

shaped slotted aperture-coupled microstrip antenna. At the first part, analyses are done for single polarized antenna.

3.3 Analysis on the Design of an Aperture-Coupled Microstrip Antenna with a Single H-Shaped Slot

As told in Section 3.2, wideband antenna is tried to be designed by using a single H-shaped slot as seen in Figure 3.19. In this section, parametrical analyses on the aperture-coupled microstrip antenna with a single H-shaped slot are performed in order to reach this wideband characteristic.

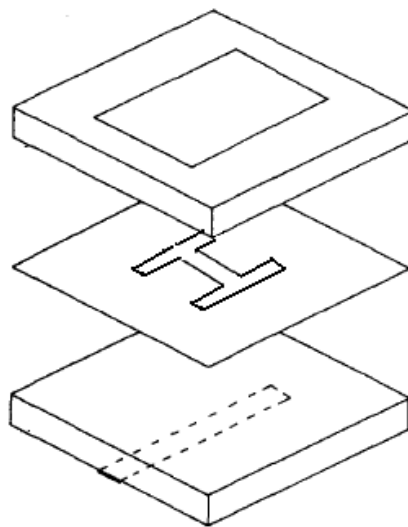


Figure 3. 19 General View of an Aperture-Coupled Microstrip Patch Antenna with a Single H-Shaped Slot.

Dielectric substrates used in the design are the same as the design of an aperture-coupled microstrip antenna with a rectangular slot, Section 3.2.

3.3.1 Parameters used in the Aperture-Coupled Microstrip Antenna Design with a Single H-Shaped Slot

There are many parameters used in the design of the aperture-coupled microstrip antenna with a single H-shaped slot. These parameters are used for increasing the

bandwidth, adjusting the resonant frequency and increasing the coupling of the antenna, so on. These parameters are shown in Figure 3.20.

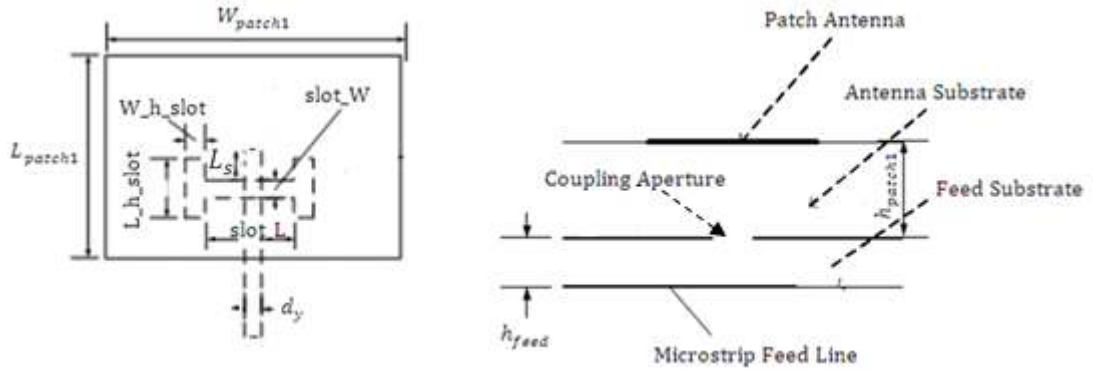


Figure 3. 20 Parameters used at the Design of an Aperture-Coupled Microstrip Antenna with a Single H-Shaped Slot.

During the design, many parameters are the same as the parameters at the design of an aperture coupled microstrip antenna with a rectangular slot. Different parameters belong to the H-shaped slot. Explanations of these new parameters are given in Table 3.2

Table 3. 2 Parameters with Explanation used in a Design of an Aperture-Coupled Microstrip Antenna with a Single H-Shaped Slot.

Name of the Parameter	Definition of the Parameter	Parameter Range	Nominal Value
L_s	Stub Length	0.5...2.5mm	1.5mm
slot_L	Length of the Slot	3.9...4.3mm	4.1 mm
slot_W	Width of the Slot	0.5...0.7mm	0.6mm
L_h_slot	Length of the Slot Edge	3...3.4mm	3.2mm
W_h_slot	Width of the Slot Edge	0.5...0.7mm	0.6mm

The parametrical analyses about the designed antenna are given in subsections below. However, the analyses about length of the microstrip patch, width of the microstrip patch, thickness of the patch substrate and slot position relative to the patch in x-direction are not given in these subsections because their effects on bandwidth and resonant frequency are same as the effects discussed in Section 3.2.

3.3.2 The Parametrical Analysis on the Stub Length

Effects of the length of the stub on resonant frequency and bandwidth characteristics are given in this section. The parametrical analysis of this variable is done between 0.5mm and 2.5mm. Return loss and bandwidth characteristics according to this parametric variation are investigated and given in Figure 3.21. In addition to this, the Smith chart plots are given in Figure 3.22.

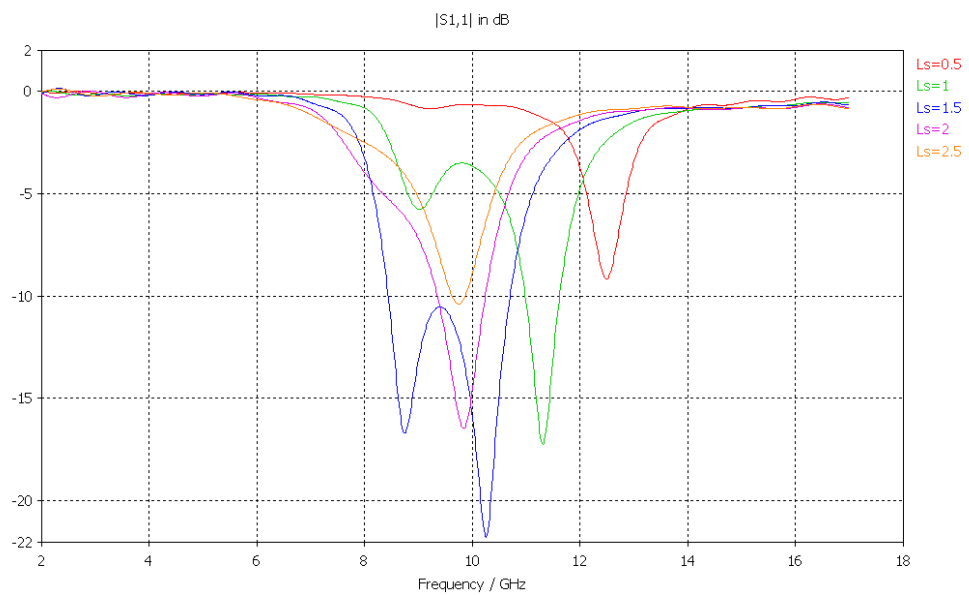


Figure 3. 21 Return Loss Parametric Analysis about the Length of the Stub of an Aperture-Coupled Microstrip Antenna with a Single H-Shaped Slot.

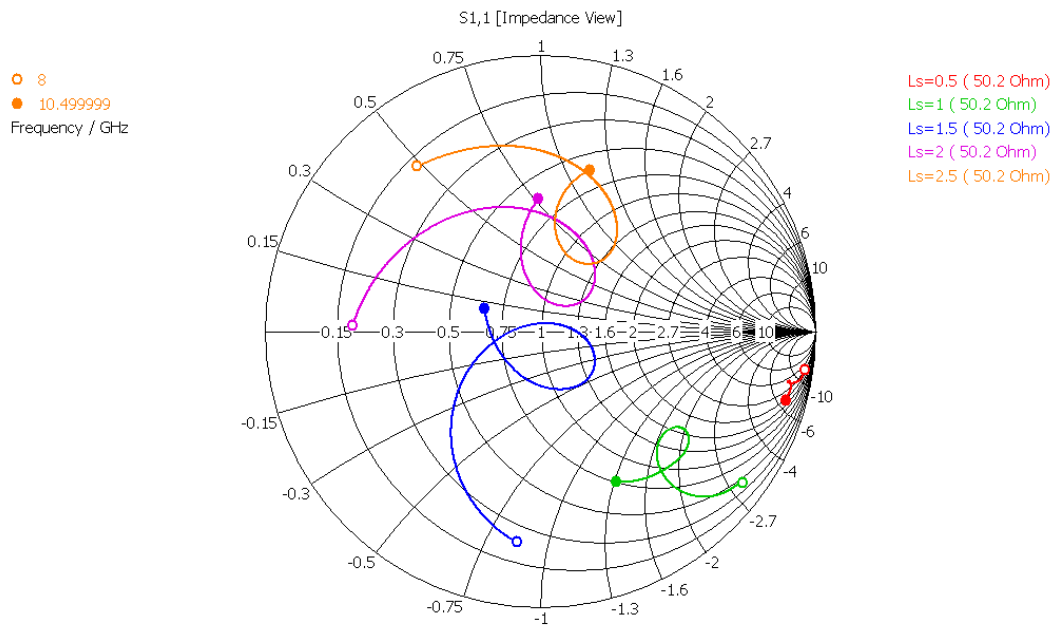


Figure 3. 22 Smith Chart of a Parametric Analysis about the Length of the Stub of an Aperture-Coupled Microstrip Antenna with a Single H-Shaped Slot.

Variations on the length of the stub change the reactance value of the antenna, so this parameter is used to adjust the excess reactance of the microstrip antenna. Therefore, matching is provided by changing this parameter. Results on the Smith Chart, Figure 3.22, show that when the length of the stub increases, the input impedance curve moves in inductive direction.

3.3.3 The Parametrical Analysis on the Length of the Center Slot

In this section, effects of the center slot length on return loss and bandwidth characteristics are given. In order to see the effects on bandwidth and return loss, the parametrical analysis on the length of the center slot is done between 3.9mm and 4.3mm. Results of this analysis are given in Figure 3.23 and the input impedance curve on Smith Chart is given in Figure 3.24.

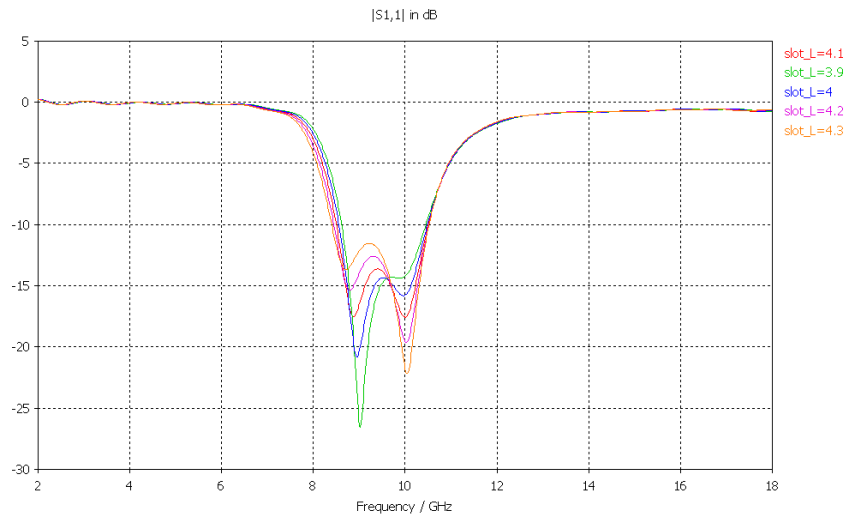


Figure 3. 23 Return Loss Parametric Analysis about the Length of the Center Slot of an Aperture-Coupled Microstrip Antenna with a Single H-Shaped Slot.

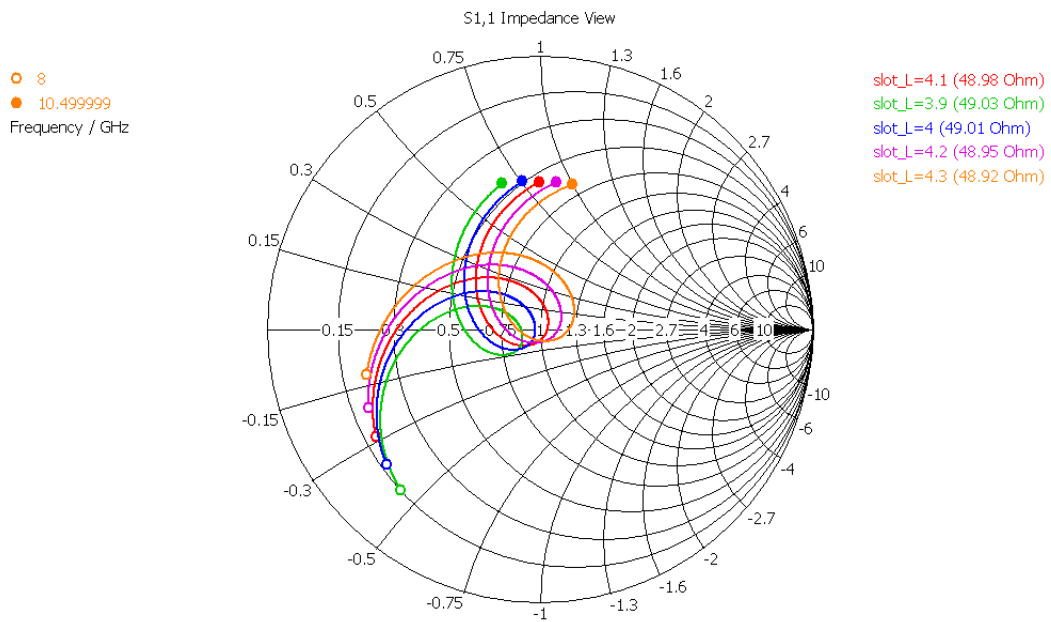


Figure 3. 24 Smith Chart of a Parametric Analysis about the Length of the Center Slot of an Aperture-Coupled Microstrip Antenna with a Single H-Shaped Slot.

It is seen from Figure 3.23 that level of coupling changes when the length of the center slot changes. If the length of the center slot increases, the resonance level becomes deeper at high frequencies. Furthermore, the diameter of the input impedance circle on Smith Chart, Figure 3.24, increases and it moves to the center of the Smith Chart when the length of the center slot increases.

3.3.4 The Parametrical Analysis on the Width of the Center Slot

This section includes the effects of the width of the center slot on return loss and bandwidth characteristics of a microstrip antenna. Analyses to see the effects of this parameter are done by changing the parameter value from 0.5mm to 0.7mm. The results of this analysis are given in Figure 3.25 and Figure 3.26.

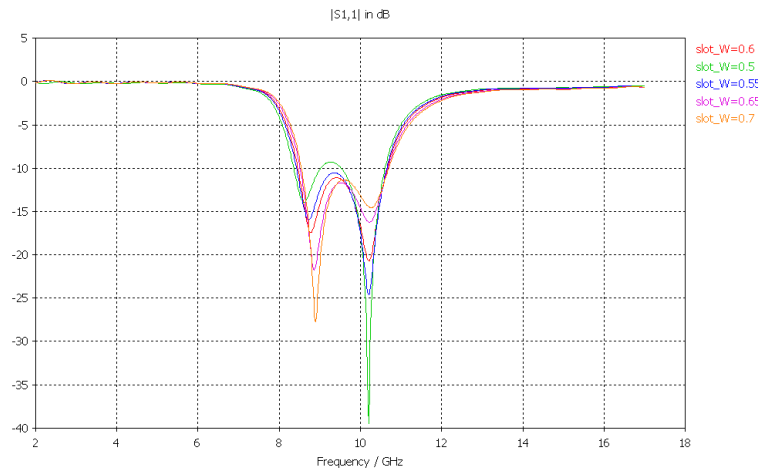


Figure 3. 25 Return Loss Parametric Analysis about the Width of the Center Slot of an Aperture-Coupled Microstrip Antenna with a Single H-Shaped Slot.

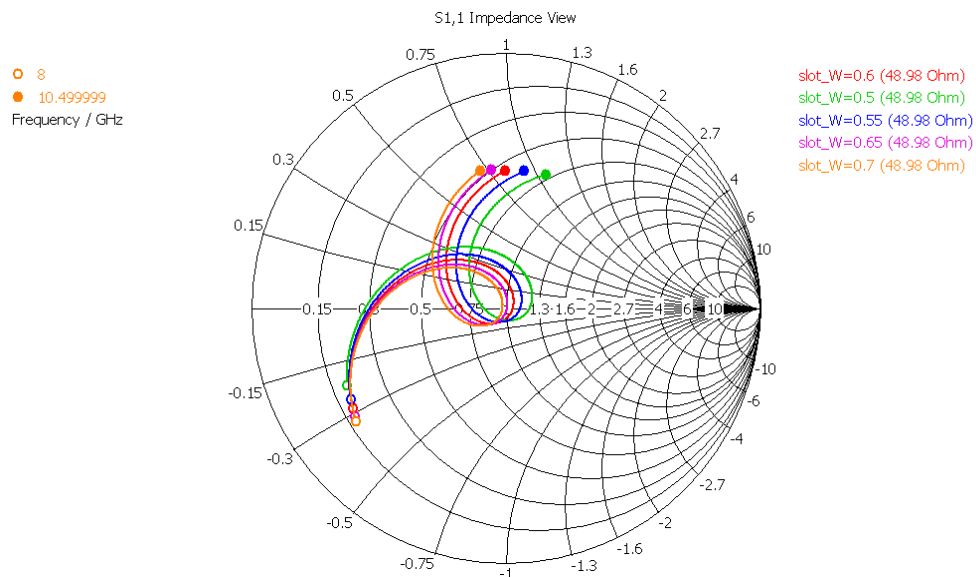


Figure 3. 26 Smith Chart of a Parametric Analysis about the Width of the Center Slot of an Aperture-Coupled Microstrip Antenna with a Single H-Shaped Slot.

The width of the center slot has also an effect on the coupling of the antenna. If the width of the center slot increases, the resonance level at high frequencies increases,

Figure 3.26. However, there exists a difference of the effect on input impedance characteristics. If the width of the center slot decreases, the input impedance circle moves to the right and there is a little change on the diameter of the circle.

3.3.5 The Parametrical Analysis on the Length of the Slot Edge

Effects of the length of the slot edge on the bandwidth are given in this section. The parametric analysis about the return loss and bandwidth is investigated by changing the length of the slot edge from 3mm to 3.4mm. Results of this analysis are given in Figure 3.27 and Figure 3.28.

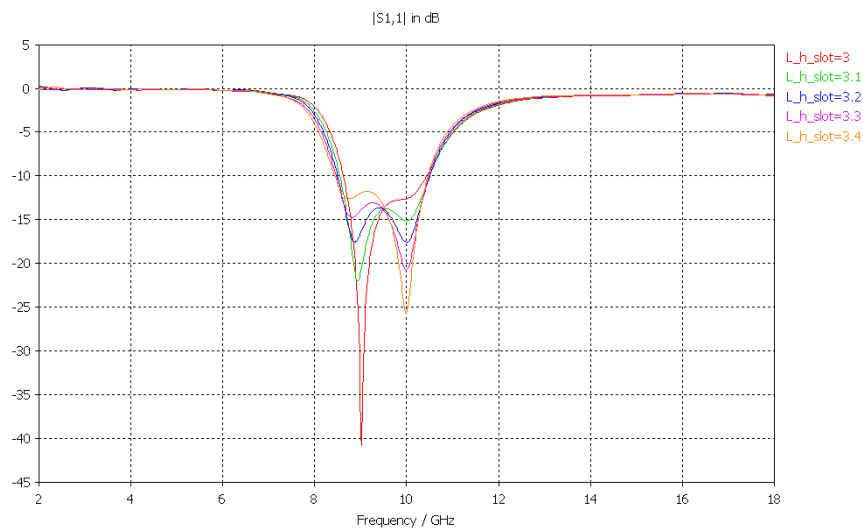


Figure 3. 27 Return Loss Parametric Analysis about the Length of the Slot Edge of an Aperture-Coupled Microstrip Antenna with a Single H-Shaped Slot.

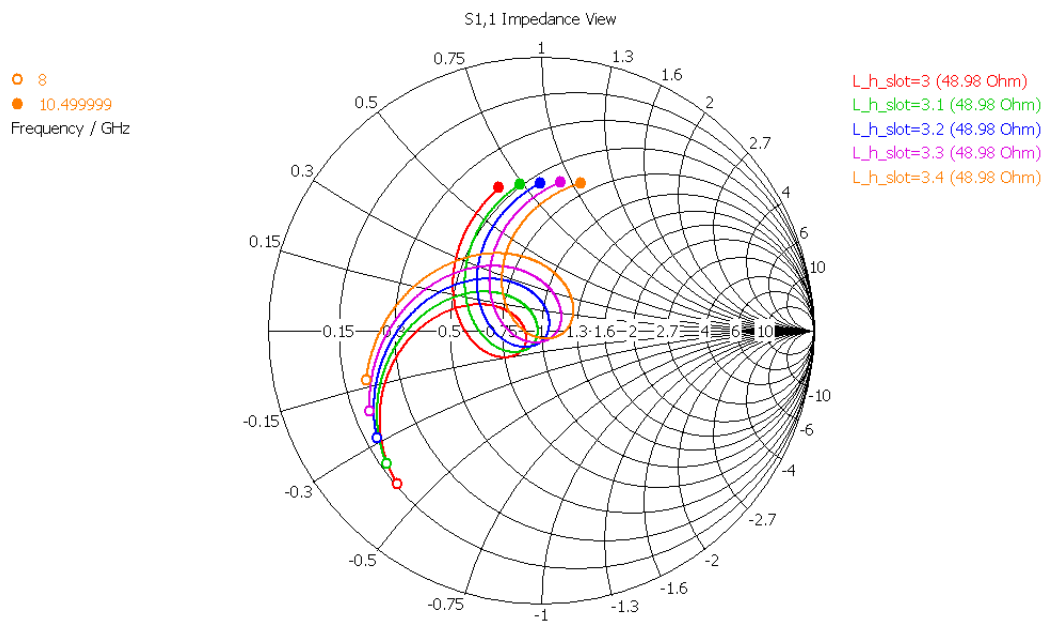


Figure 3. 28 Smith Chart of a Parametric Analysis about the Length of the Slot Edge of an Aperture-Coupled Microstrip Antenna with a Single H-Shaped Slot.

Variations on the length of the slot edge have an effect on the coupling of the microstrip antenna. The return loss level and resonance frequency of the antenna change when the parameter varies. The variations on this parameter show similar effects as the variations on the length of the center slot, as seen in Figure 3.27. Moreover, this parameter has an effect on the input impedance of the antenna. The Smith Chart on the Figure 3.28 shows that when the length of the slot edge increases, the diameter of the circle increases and it moves towards the inductive direction.

3.3.6 The Parametrical Analysis on the Width of the Slot Edge

In this section, effects of the variation for the width of the slot edge on bandwidth are given. The parametric analysis is done by varying this parameter from 0.5mm to 0.7mm. Like the length of the slot edge, the width of the slot edge affects the coupling level of the microstrip antenna. The variations on this parameter show similar effects as the variations on the width of the center slot, as seen in Figure

3.29. At the Smith Chart, Figure 3.30, the diameter of the circle increases and the circle moves to inductive direction when the width of the edge slot increases.

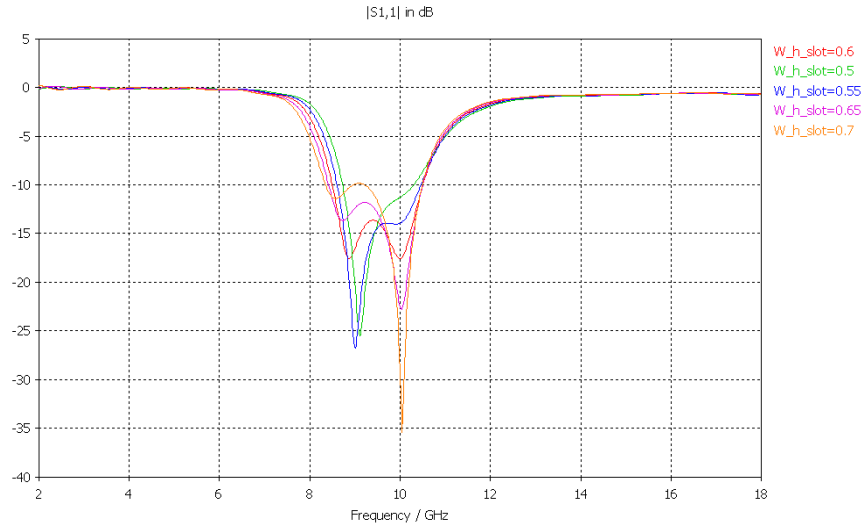


Figure 3. 29 Return Loss Parametric Analysis about the Width of the Slot Edge of an Aperture-Coupled Microstrip Antenna with a Single H-Shaped Slot.

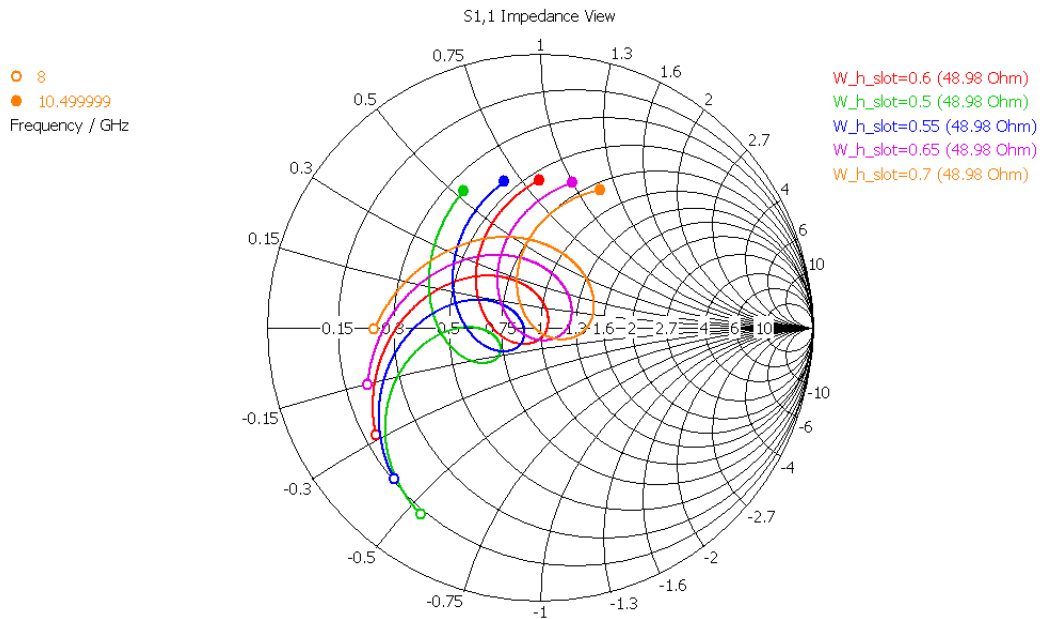


Figure 3. 30 Smith Chart of a Parametric Analysis about the Width of the Slot Edge of an Aperture-Coupled Microstrip Antenna with a Single H-Shaped Slot.

All of these analyses are taken into account in order to design an aperture-coupled microstrip antenna with a bandwidth of 20%. Length of the slot on the aperture

becomes smaller than the designed antenna with a rectangular slot as seen from Table 3.3.

Table 3. 3 Parameters of a Designed Aperture-Coupled Microstrip Antenna with a Single H-Shaped Slot.

Name of the Parameter	Value of the Parameter for H-shaped Slot	Value of the Parameter for Rectangular Slot
La	50mm	50mm
Wa	50mm	50mm
L_patch1	9.9mm	9.9mm
W_patch1	9.9mm	9.9mm
Ls	1.5mm	1.9mm
dy	1.1mm	1.1mm
h_feed	0.508mm	0.508mm
h_patch1	2.5mm	2.5mm
slot_L	5.3mm	8.7mm
slot_W	0.6mm	0.6mm
L_h_slot	3.2mm	-
W_h_slot	0.6mm	-
x_slot	0mm	0mm
y_slot	0mm	0mm
ϵ_{rf}	3.55	3.55
ϵ_{ra}	1.025	1.025

Return loss and bandwidth characteristic of a designed aperture-coupled microstrip antenna with an H-shaped slot is given in Figure 3.31.

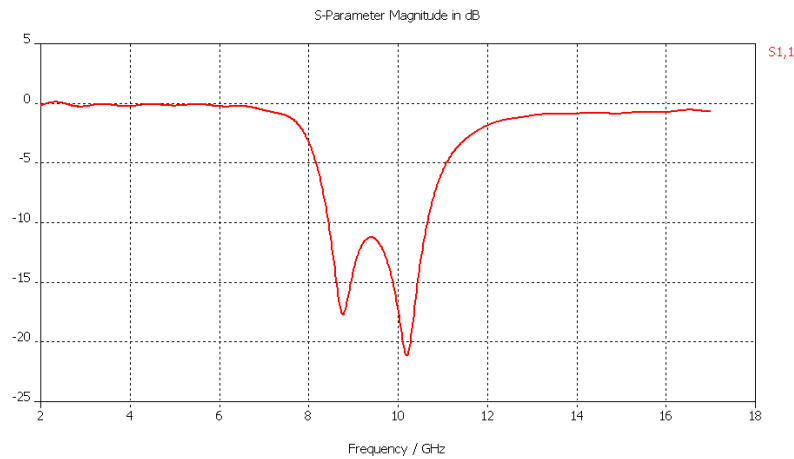


Figure 3. 31 Return Loss Analysis for a Designed Aperture-Coupled Microstrip Antenna with a Single H-Shaped Slot.

If Figure 3.19 and Figure 3.31 are compared, it can be observed that approximately the same bandwidth is achieved with a shorter slot with H-shaped aperture (Table 3.3). For dual-polarization operation, two orthogonal slots need to be placed under the patch which is not a possible configuration with rectangular slots due to their long dimensions. However, due to the reduction achieved in the length of the slot, this configuration may be possible through the use of H-shaped slots. H-shaped slots have two length parameters. One of them is the length of the center slot and the other is the length of the edge slots. It would be easier to place the two orthogonal slots within the area of the patch if the two slots have different aspect ratios such that one of the slots is longer at the center and the other one is longer at the edges. As a result, one more analysis is performed to explore the possibility of designing two different antennas with similar characteristics but with different slot parameters. At the end of this analysis, two different antennas are designed. The dimensions of the H-shaped slots used in these antennas are compared in Figure 3.32. The return loss characteristics of these antennas are compared in Figure 3.33. It can be observed that similar characteristics can be obtained with slots that have different aspect ratios.

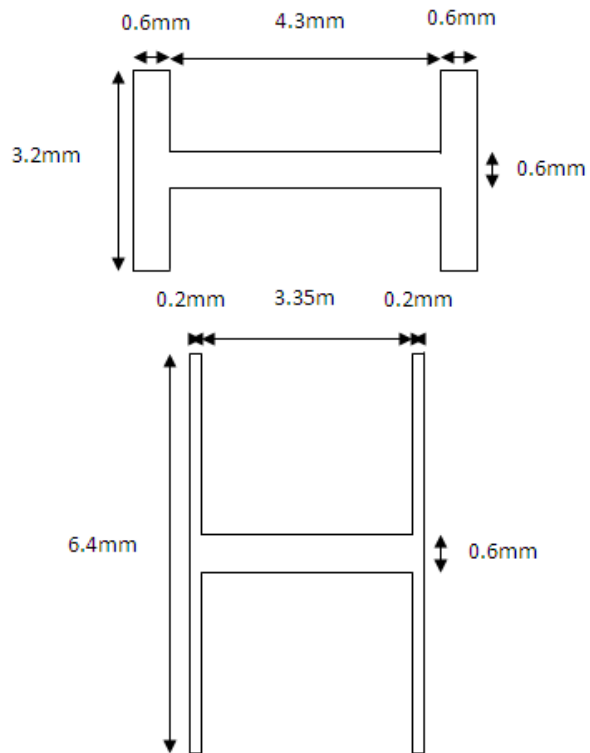


Figure 3. 32 Lengths and Widths of Two H-Shaped Slots.

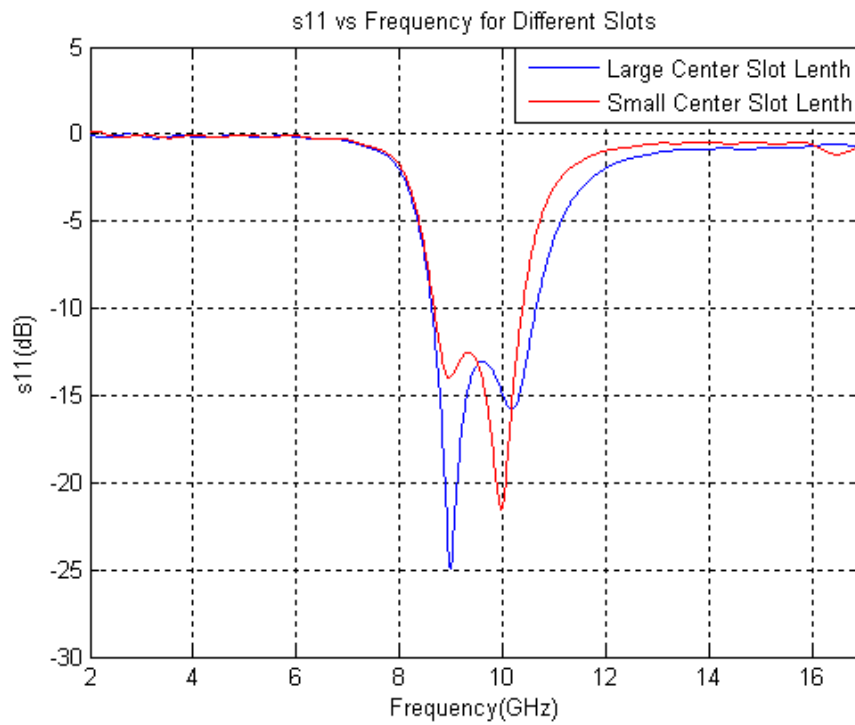


Figure 3. 33 Return Loss Analysis for Two H-Shaped Slots.

Therefore, it is seen that dual-polarized antenna can be designed with two orthogonal H-shaped slots. The design requirements are that the wideband characteristic should be supplied for each polarization and the mutual coupling between the microstrip feeds should be as small as possible.

3.4 Analyses on the Design of a Dual-Polarized Aperture-Coupled Microstrip Antenna with H-Shaped Slots

General view of the dual-polarized aperture-coupled microstrip antenna with H-shaped slots is given in Figure 3.34.

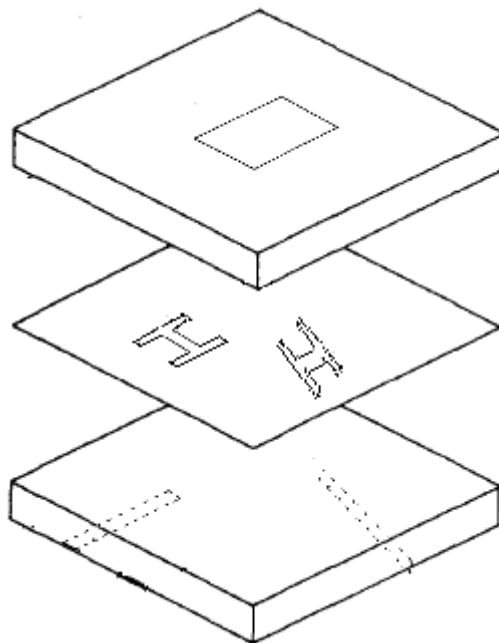


Figure 3. 34 General View of an Aperture-Coupled Microstrip Patch Antenna with Two Orthogonally Placed H-Shaped Slots.

The parameters used during the design of a dual-polarized aperture-coupled microstrip antenna are defined in Figure 3.35.

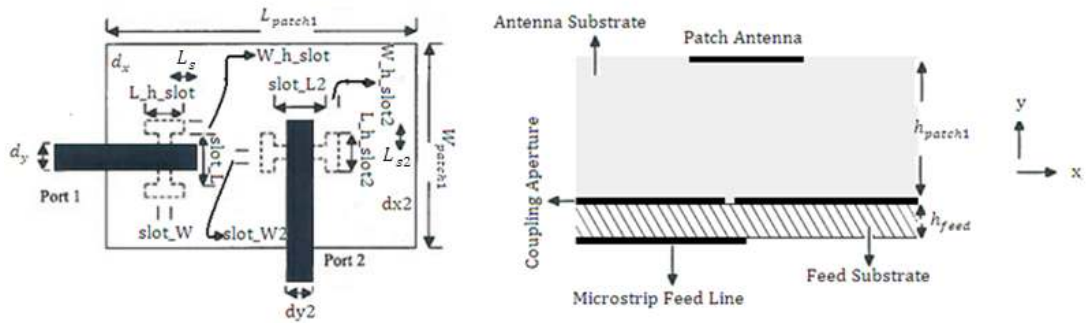


Figure 3.35 Parameters used at the Design of an Aperture-Coupled Microstrip Antenna with Two Orthogonally Placed H-Shaped Slots.

The H-shaped slot designed in Section 3.3 is used at port 1 for the design of dual-polarized application and this slot is moved in $-x$ direction. This movement of the slot gives a possibility to place a second slot orthogonal to the first slot. Movement in the $-x$ direction changes the return loss characteristic of the antenna, so the parameters are altered to provide the required bandwidth. For good coupling, slots should be placed at the bottom part of the microstrip patch borders, so two orthogonal slots should come closer to provide this. However, mutual coupling between the slots should be kept in lower values. In order to place two slots efficiently, length of the center slot is selected as large for port 1 and length of the center slot is selected as small for port 2. In addition, length of the slot edge is selected as small for port 1 and length of the slot edge is selected as large for port 2. Therefore, high coupling and less mutual coupling are tried to be provided by adjusting these parameters.

All of these analyses are done in order to design a dual-polarized aperture-coupled microstrip antenna with a bandwidth of 20%. Values of the designed antenna parameters for orthogonal feed line and slots are given in Table 3.4.

Table 3. 4 Parameters of a Designed Aperture-Coupled Microstrip Antenna with Two Orthogonally Placed H-Shaped Slots.

Name of the Parameter	Value of the Parameter
L_s	1.4mm
L_{s2}	1.3mm
slot_L	4.15mm
slot_L2	3.15mm
slot_W	0.6mm
slot_W2	1.1mm
L_h_slot	3.5mm
L_h_slot2	6mm
W_h_slot	0.65mm
W_h_slot2	0.4mm
x_slot	-2.5mm
x_slot2	2.5mm
y_slot	0mm
y_slot2	0mm

Return loss and bandwidth characteristics for two ports for the designed dual-polarized aperture-coupled microstrip antenna are shown in Figure 3.36 and Figure 3.37. Furthermore, the isolation between two ports is also given in Figure 3.38.

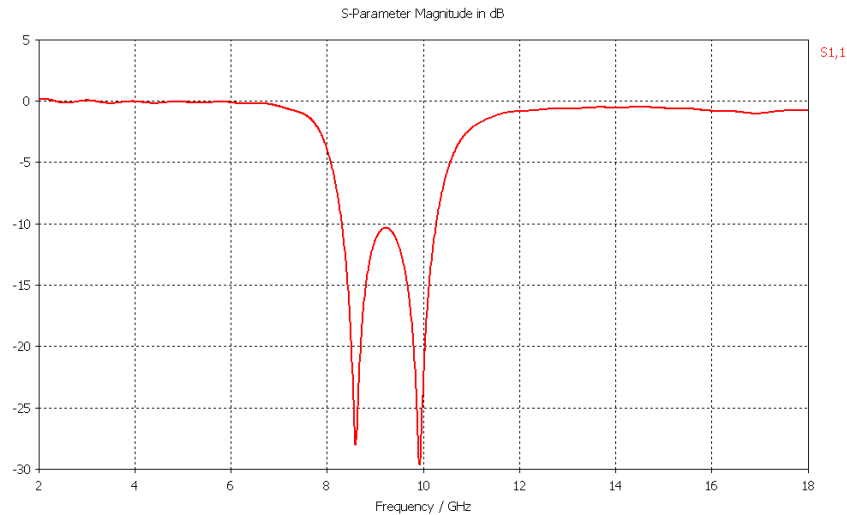


Figure 3. 36 Return Loss Graph of Port 1 for a Designed Dual-Polarized Aperture-Coupled Microstrip Antenna with H-Shaped Slots.

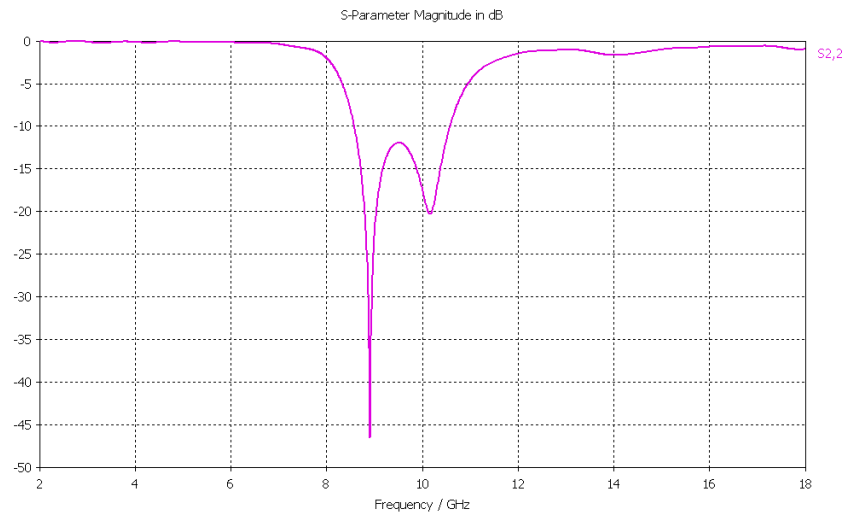


Figure 3. 37 Return Loss Graph of Port 2 for a Designed Dual-Polarized Aperture-Coupled Microstrip Antenna with H-Shaped Slots.

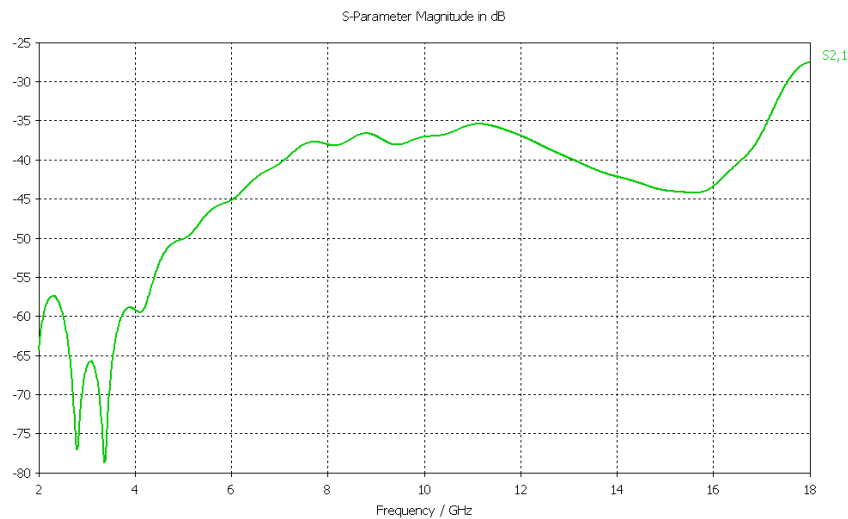


Figure 3. 38 Isolation between Ports for a Designed Dual-Polarized Aperture-Coupled Microstrip Antenna with H-Shaped Slots.

Figures 3.36-3.38 show that wide bandwidth characteristic is provided in dual-polarized aperture-coupled microstrip antenna by using H-shaped slots on aperture. In addition, insertion loss between ports is in the acceptable values, $< -25\text{dB}$.

CHAPTER 4

FABRICATION AND MEASUREMENT OF A DUAL-POLARIZED APERTURE-COUPLED MICROSTRIP ANTENNA

After investigating the analysis done in Chapter 3, the antenna with the optimized parameter values is fabricated. Pictures of the produced parts of the antenna and the produced antenna is given is Figure 4.1.

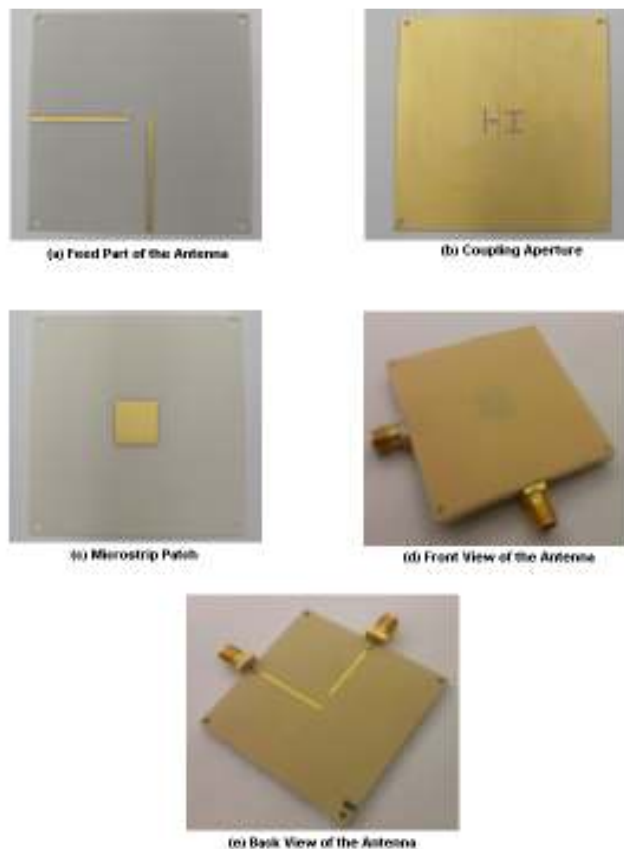


Figure 4. 1 Parts and Total Structure of the Dual-Polarized Aperture-Coupled Microstrip Antenna with a Single Patch.

After the production of the antenna is completed, return loss values are measured and compared with simulation results. Comparison results are given in Figure 4.2 for two ports.

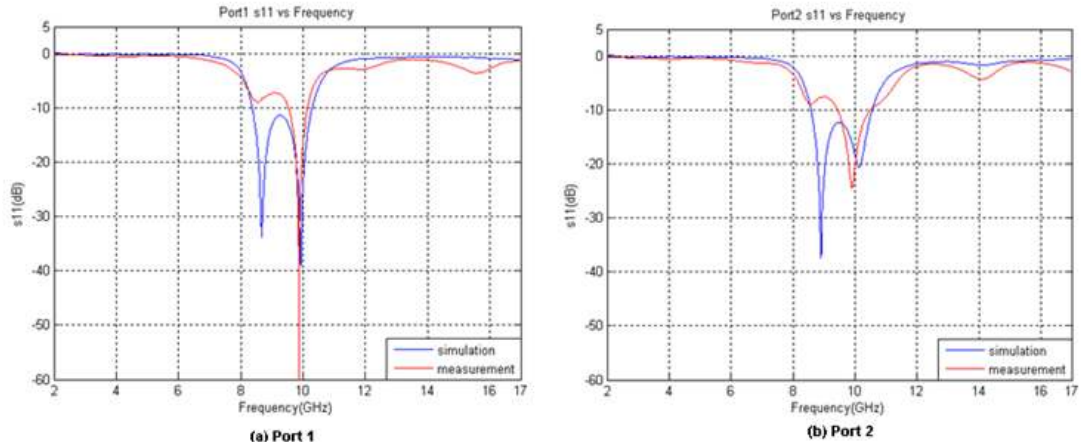


Figure 4. 2 Return Loss Comparisons between Fabricated and Simulated Dual-Polarized Aperture-Coupled Microstrip Antennas with a Single Patch for Port 1 and Port 2.

As seen from Figure 4.2, there exist differences in return loss characteristics between simulated and fabricated antennas. The return loss level between two resonances is increased for both ports in the measurement phase of the antenna. The reason of this is that there exists a mismatch when the microstrip feed line is fed with a connector. In order to eliminate this problem, stubs are connected to the microstrip feed line. The reason is that open stubs destroy the reactance values coming from the connector mismatch. Figure of the used stubs and their effect on return loss level, by comparison with the measurement graph without stubs and simulation graph, is shown in Figure 4.3 and Figure 4.4.

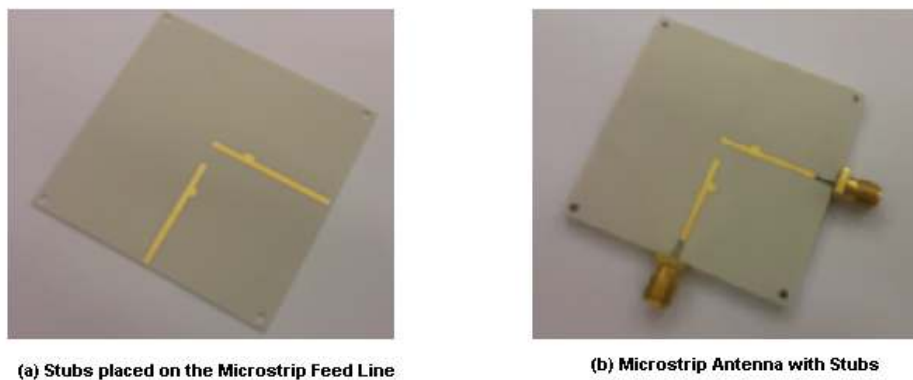


Figure 4. 3 Fabricated Microstrip Feed Line and Microstrip Antenna with Open-Circuited Stubs.

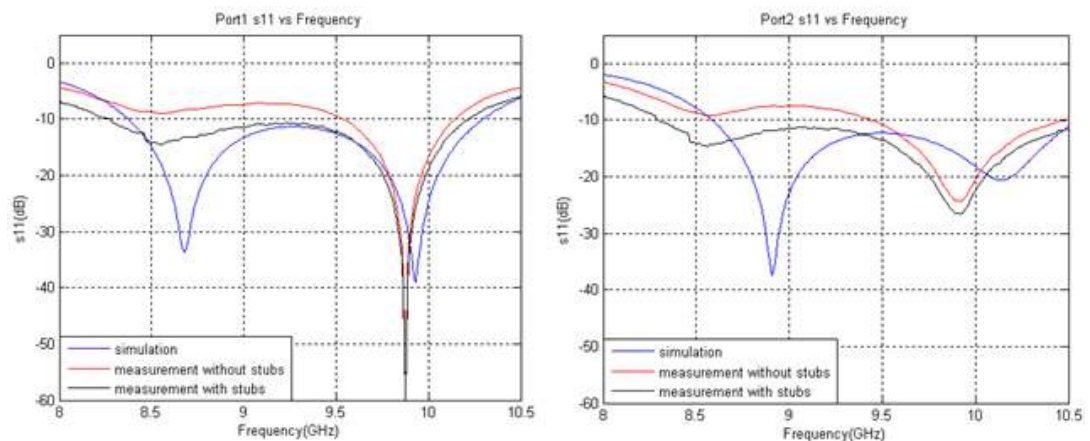


Figure 4. 4 Return Loss Comparison between Fabricated and Simulated Antennas with and without stubs for Port 1 and Port 2.

As seen from Figure 4.4, the open-circuited stubs compensate the reactance value coming from the input connectors, so simulation and measurement results resemble each other and bandwidth requirement is observed to be satisfied.

After the bandwidth requirement of the antenna is satisfied, far field patterns of the antenna for both ports are investigated. The measurement set-up is shown in Figure 4.5.



Figure 4. 5 Far Field Pattern Measurement Set-up.

Measurements are done by using SATIMO Starlab Spherical Nearfield Measurement System and they are compared with simulation results. Comparisons about the far field patterns, E-planes, are given in Figure 4.6.

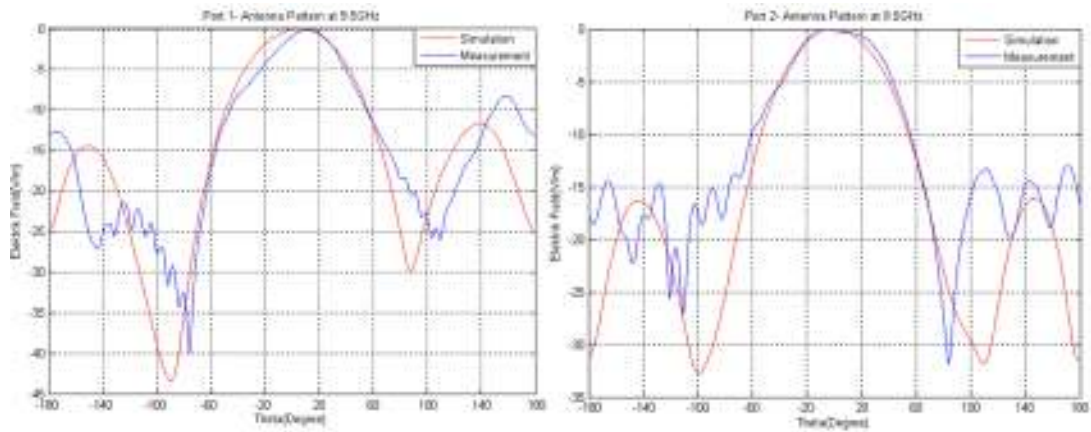


Figure 4. 6 Far Field Pattern Comparisons between Simulation and Measurement at both Ports.

It is seen that, there exists back lobes for both ports of the antenna due to the slots. This problem can be eliminated by placing a metal plate at the back part of the antenna. It should also be noted that the front to back ratio is better for Port 2, since the H-shaped slot at Port 2 is the one that has shorter center slot.

CHAPTER 5

IMPEDANCE CALCULATION OF A MICROSTRIP LINE FED H-SHAPED SLOT

Geometry of a slot fed by a microstripline is given in Figure 5.1. At this configuration, infinite microstripline lies on the x-direction and slot lies in y-direction on the dielectric substrate. This slot can be modeled as a series impedance on the microstrip line. The impedance of the slot can be calculated by considering only a single dominant mode propagating under the microstrip line and by neglecting the effects of higher order modes.

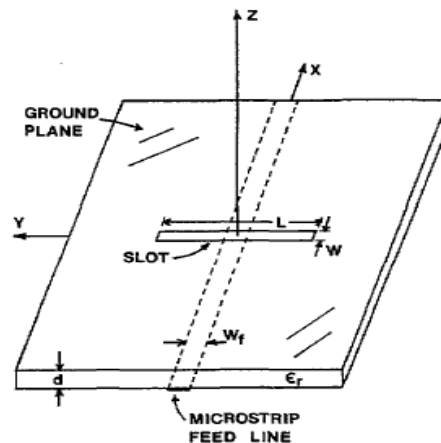


Figure 5. 1 Geometry of Slot fed by a Microstripline [30].

Dominant mode of a microstrip line can be considered as a quasi-transverse electromagnetic mode (TEM mode). The slot at $x=0$ creates a discontinuity and total microstrip line fields (\vec{E}) can be written in terms of positive (\vec{E}^+) and negative (\vec{E}^-) traveling fields as:

$$\begin{aligned}\bar{E} &= \begin{cases} \bar{E}^+ + R\bar{E}^-, & \text{for } x < 0 \\ T\bar{E}^+ & , \text{for } x > 0 \end{cases} \\ \bar{H} &= \begin{cases} \bar{H}^+ + R\bar{H}^-, & \text{for } x < 0 \\ T\bar{H}^+ & , \text{for } x > 0 \end{cases}\end{aligned}\quad (5.1)$$

In equation 5.1, R and T are the reflection and the transmission coefficients on the line, respectively. At this stage, reciprocity theorem can be utilized to find R and T [30]. R can be obtained by applying reciprocity theorem for the total fields and positive traveling fields as:

$$\int_S \bar{E} \times \bar{H}^+ \cdot dS = \int_S \bar{E}^+ \times \bar{H} \cdot dS \quad (5.2)$$

The closed surface S in equation 5.2 consists of three sections. First one is the cross section of the microstrip line, second surface is the ground plane ($z=0$ plane) and the third surface which is denoted as S_w is called as the walls of the microstrip line and it extends to $\pm \infty$ in y direction and it extends from 0 to ∞ in z direction. $\hat{n} \times \bar{E}$ on S_w is 0 for both total field and positive travelling wave. The integral over the ground plane surface is limited by the area of the aperture, S_a , since the tangential electric field is zero on the conducting plate. $\hat{n} \times \bar{E}^+$ is equal to zero on aperture surface; however, $\hat{n} \times \bar{E}$ is equal to $V_0 \hat{n} \times \hat{x} e_x^a$ where $V_0 e_x^a$ is the unknown aperture field. Therefore, reflection coefficient can be found as:

$$R = \frac{V_0}{2} \int_{S_a} e_x^a(x, y) h_y(x, y) dS \quad (5.3)$$

Where h_y is the quasi-TEM magnetic field mode excited by the microstrip feed line.

To simplify the expressions, discontinuity voltage (Δv) can be defined as:

$$\Delta v = \int_{S_a} e_x^a(x, y) h_y(x, y) dS \quad (5.4)$$

T can be obtained by applying reciprocity theorem for the total fields and negative traveling fields as:

$$\int_S \bar{E} \times \bar{H}^- \cdot dS = \int_S \bar{E}^- \times \bar{H} \cdot dS \quad (5.5)$$

Transmission coefficient can be found by using equation 5.5:

$$T = 1 - \frac{V_0}{2} \int_{S_a} e_x^a(x, y) h_y(x, y) dS = 1 - R \quad (5.6)$$

The relation between T and R obtained in equation 5.6 implies that the slot on the microstrip feed line can be modeled as a series impedance.

In order to find R and T values, V_0 has to be found. This variable is found by enforcing the continuity of the tangential component of the magnetic field at the aperture. These fields are:

H_y^e is the field at $z < 0$ due to $V_0 e_x^a$

H_y^i is the field at $z > 0$ due to $V_0 e_x^a$

H_y^f is the field at $z > 0$ due to microstrip feed line modes

From the magnetic fields above, equation 5.7a can be written:

$$H_y^e = H_y^f + H_y^i \quad (5.7a)$$

Interior fields due to feed line modes at $x = 0^-$ can be written as:

$$H_y^f = (1 - R) h_y \quad (5.7b)$$

From equations 5.7a and 5.7b, magnetic fields on both sides of the slot can be written as:

$$H_y^e - H_y^i = (1 - R) h_y \quad (5.7c)$$

Magnetic fields on slot can be calculated by using the corresponding Green's function on the left side of equation 5.7c.

$$V_0 \int_{S_a} G_{yy}^{HM}(x, y; x_0, y_0) \cdot e_x^a(x_0, y_0) ds_0 = (1 - R) h_y(x, y) \quad (5.7d)$$

In equation 5.7d, G_{yy}^{HM} is the Green's function for y-directed H field at $z=0$ due to a y-directed magnetic current source at $z=0$.

Equation 5.7d can be enforced in the average sense by testing both sides of the equation with $e_x^a(x, y)$ and consequently the following equation is obtained.

$$\begin{aligned} V_0 \int_{S_a} \int_{S_a} e_x^a(x, y) G_{yy}^{HM}(x, y; x_0, y_0) \cdot e_x^a(x_0, y_0) ds ds_0 &= (1 - R) \int_{S_a} e_x^a(x, y) h_y(x, y) ds \\ &= (1 - R) \Delta v \end{aligned} \quad (5.7e)$$

By defining a new variable Y^e as:

$$Y^e = \int_{S_a} \int_{S_a} e_x^a(x, y) G_{yy}^{HM}(x, y; x_0, y_0) \cdot e_x^a(x_0, y_0) ds ds_0 \quad (5.7f)$$

All three unknowns of the problem can be found as:

$$V_0 = \frac{2\Delta v}{\Delta v^2 + 2Y^e} \quad (5.7g)$$

$$R = \frac{\Delta v^2}{\Delta v^2 + 2Y^e} \quad (5.7h)$$

$$T = \frac{2Y^e}{\Delta v^2 + 2Y^e} = 1 - R \quad (5.7i)$$

Finally, the series impedance can be calculated as:

$$Z = Z_c \frac{2R}{1 - R} \quad (5.7j)$$

If a rectangular slot is analyzed by using this technique, a sinusoidal electric field distribution can be assumed over the aperture (e_x^a), and the series impedance value can be calculated quite accurately by using this trial function. However, one of the objectives of this thesis is to apply this technique in the analysis of slots with different shapes. In that case, the electric field distribution (or the magnetic current density) on the aperture becomes unknown and it needs to be expanded in terms of known basis functions. In this thesis, roof-top basis functions, which are triangular in the direction of current and constant in the plane perpendicular to the current flow, are used. When e_x^a is expanded in terms of basis functions, $e_x^a \approx \sum_n V_n e_{xn}^a$, the

discontinuity voltage, Δv , becomes a vector and the admittance parameter, Y^e becomes a matrix. The entries of discontinuity voltage vector and the admittance matrix can be calculated by using the following expressions:

$$\Delta v_n = \int_{S_a} e_{x_n}^a(x, y) h_y(x, y) ds \quad (5.8a)$$

$$Y_{mn}^e = \int_{S_a} \int_{S_a} e_{x_m}^a(x, y) G_{yy}^{HM}(x - x_0, y - y_0) e_{x_n}^a(x_0, y_0) ds ds_0 \quad (5.8b)$$

The unknown coefficients of the aperture field distribution can be found as:

$$[V] = \left\{ [Y^e] + \frac{1}{2} [\Delta v][\Delta v]^t \right\}^{-1} [\Delta v] \quad (5.8c)$$

Finally, the reflection coefficient is calculated as:

$$R = \frac{1}{2} [V]^t [\Delta v] \quad (5.8d)$$

At the equation 5.8b, it is seen that two surface integrals have to be calculated in order to find a solution. However, this calculation takes a long time, so in order to reduce the computation time, change of variables technique is used and (5.8b) is written as:

$$\int \int G_{yy}^{HM}(u, v) \int \int e_{x_m}(u + x_0, v + y_0) e_{x_n}(x_0, y_0) dx_0 dy_0 dudv \quad (5.9)$$

The inner integral (correlation of basis and testing function $T \otimes B$) in equation 5.9 is performed analytically by using the symbolic math tool of MATLAB. In order to be able to develop a versatile code, the sizes of basis functions are not limited to be equal to each other. Consequently, the basis and testing functions may span domains with different lengths. Each triangle is a combination of two half triangles that may have different lengths. Therefore the correlation integral can be written as a summation of four ($2 \times 2 = 4$) integrals. The limits and integrands of each correlation integral that will be evaluated analytically are found by the help of the figures given

in the Appendix. The remaining outer integral is calculated numerically by using Gaussian Quadrature technique.

The spatial domain Green's function G_{yy}^{HM} , can be written in terms of its spectral domain counterpart, \tilde{G}_{yy}^{HM} , by using the following Fourier Transform integral.

$$G_{yy}^{HM} = \frac{1}{4\pi^2} \iint_{-\infty}^{\infty} \tilde{G}_{yy}^{HM}(k_x, k_y) e^{jk_x(x-x_0)} e^{jk_y(y-y_0)} dk_x dk_y \quad (5.10a)$$

where

$$\tilde{G}_{yy}^{HM} = \frac{-j}{k_0 Z_0} \left[\frac{j(k_1 \cos k_1 d + jk_2 \varepsilon_r \sin k_1 d) (\varepsilon_r k_0^2 - k_y^2)}{k_1 T_m} - \frac{jk_y^2 k_1 (\varepsilon_r - 1)}{T_e T_m} - \frac{k_0^2 - k_y^2}{jk_2} \right] \quad (5.10b)$$

$$T_e = k_1 \cos k_1 d + jk_2 \sin k_1 d \quad (5.10c)$$

$$T_m = \varepsilon_r k_2 \cos k_1 d + jk_1 \sin k_1 d \quad (5.10d)$$

$$k_1^2 = \varepsilon_r k_0^2 - \beta^2, \quad \text{Im } k_1 < 0 \quad (5.10e)$$

$$k_2^2 = k_0^2 - \beta^2, \quad \text{Im } k_2 < 0 \quad (5.10f)$$

$$\beta^2 = k_x^2 + k_y^2 \quad (5.10g)$$

$$k_0^2 = w^2 \mu_0 \varepsilon_0 = (2\pi/\lambda_0)^2 \quad (5.10h)$$

$$Z_0 = \sqrt{\mu_0/\varepsilon_0} \quad (5.10i)$$

The integral in (5.10a) can not be evaluated analytically. In order to avoid the numerical integration of this integral, Discrete Complex Image Method (DCIM) [35] is utilized. In this method, first the spectral domain Green's function is approximated by a summation of complex exponentials as:

$$\tilde{G} = \sum_i \frac{\beta_i e^{\alpha_i k_z}}{jk_z} \quad (5.11a)$$

Then by using the following relation, the spatial domain Green's function can be easily calculated.

$$\frac{e^{-jkr}}{r} = \frac{1}{\pi} \iint_{-\infty}^{\infty} dk_x dk_y e^{-j(k_x x + k_y y)} \frac{e^{-jk_z |z|}}{2jk_z} \quad (5.11b)$$

From (5.11a), the spatial domain Green's function, G , can be written as;

$$G = \frac{1}{2\pi} \sum_i \beta_i \frac{e^{-jk_0 r_i}}{r_i} \quad (5.11c)$$

where

$$r_i = \sqrt{(x - x_0)^2 + (y - y_0)^2 - \alpha_i^2} \quad (5.11d)$$

Note that there exists k_y^2 terms in the spectral domain Green's function expressions given in (5.10b). While implementing The DCIM to approximate this Green's function, two different sets of exponents and coefficients are obtained. The first set corresponds to terms without k_y^2 factor and the second set corresponds to the terms which are multiplied by k_y^2 . Consequently, (5.10a) is approximated as:

$$\tilde{G}_{yy}^{HM} = \sum_i \frac{\beta_i^1 e^{\alpha_i^1 k_z}}{jk_z} - k_y^2 \sum_i \frac{\beta_i^2 e^{\alpha_i^2 k_z}}{jk_z} \quad (5.12)$$

The corresponding Green's function in spatial domain is obtained by using the identity that multiplication by $-jk_y$ in the spectral domain corresponds to taking the derivative with respect to y in the spatial domain. Then the second order derivative with respect to y is transferred onto the basis and testing functions during the evaluation of Y^e matrix entries. Therefore, the evaluation of correlation integrals for the derivatives of basis and testing functions are also included in the Appendix.

The quasi-TEM mode magnetic field excited by the microstrip line, $h_y(x, y)$, needs to be evaluated to calculate the discontinuity voltage vector. It can be calculated as:

$$h_y = \frac{1}{\sqrt{Z_c}} \frac{1}{2\pi} \int_{-\infty}^{\infty} F_u(k_y) \tilde{G}_{yx}^{HJ}(-\beta, k_y) e^{-j\beta x} e^{jk_y y} dk_y \quad (5.13a)$$

where

$$F_u(k_y) = \frac{\sin k_y \frac{W}{2}}{k_y \frac{W}{2}} \quad (5.13b)$$

and

$$\tilde{G}_{yx}^{HJ} = \frac{-jk_x^2(\epsilon_r - 1) \sin k_1 d}{T_e T_m} + \frac{k_1}{T_e} \quad (5.13c)$$

At the equations (5.13b) and (5.13c), $F_u(k_y)$ is the Fourier Transform of a pulse of width W .

G_{yx}^{HJ} is the Green's function for y component of the magnetic field at $(x, y, 0)$ due to a \hat{x} directed electric current element at (x_0, y_0, d) [30].

DCIM method is also utilized for the efficient computation of, $h_y(x, y)$, by using the following identity.

$$H_0^2(k\rho) = \frac{1}{\pi} \int_{-\infty}^{\infty} dk_x \frac{e^{-jk_x x - jk_y |y|}}{k_y} \quad (5.14a)$$

where

$$k_x^2 + k_y^2 = k^2 \quad (5.14b)$$

$$x^2 + y^2 = \rho^2 \quad (5.14c)$$

First the integrand of (5.13a) is approximated by a summation of complex exponentials as:

$$\frac{\sin k_y W/2}{k_y W/2} \tilde{G}_{yx}^{HJ}(-\beta, k_y) \approx \sum_i \beta_i \frac{e^{jk_z \alpha_i}}{k_z} \quad (5.15)$$

where

$k_z = k_1$ where k_1 is the wave number of dielectric material.

Then, the normalized magnetic field of the microstrip line is written as:

$$h_y = \frac{1}{2\sqrt{Z_c}} \sum_i \beta_i H_0^2 \left(k_t \sqrt{y^2 - \alpha_i^2} \right) e^{-j\beta x} \quad (5.16a)$$

where

$$k_t = \sqrt{k_z^2 + k_y^2} = \sqrt{k^2 - \beta^2} \quad (5.16b)$$

The coefficients of the exponentials and the exponents used in the approximation of the Green's functions are obtained from the codes developed by Mustafa İncebacak during his M. Sc. Studies [73].

Singularity Extraction Problem

Let us recall the integral involved in the evaluation of the admittance matrix.

$$Y_{mn}^e = \int_{S_a} \int_{S_a} e_{xm}^a(x, y) G_{yy}^{HM}(x - x_0, y - y_0) e_{xn}^a(x_0, y_0) ds ds_0 \quad (5.8b)$$

A singularity problem exists when the observation point (domain of the test function) coincides with the source point (domain of the basis function) [31]. In order to avoid singularity problem, the singularity extraction method is applied in this thesis. Since the Green's function is approximated as a summation of spherical exponentials, the singularity extraction formulation can be derived by considering the free space Green's function. The Taylor series expansion of exponential function can be used as follows:

$$\frac{e^{-jkR}}{R} = \frac{1 - jkR - \frac{k^2 R^2}{2} + \frac{jk^3 R^3}{6} \dots}{R} \cong \frac{1}{R} - jk \quad (5.17a)$$

By using the Taylor series expansion the integral equation for the correlation of test and base functions can be decomposed into two parts as follows:

$$\int \frac{e^{-jkR}}{R} (T \otimes B) dudv = \underbrace{\int -jk(T \otimes B) dudv}_{\text{numerical}} + \underbrace{\int \frac{1}{R} (T \otimes B) dudv}_{\text{analytical}} \quad (5.17b)$$

Since no singularity exists for the first integral, it can be evaluated numerically. However, the second integral that involves $1/R$ singularity, needs to be evaluated analytically. As discussed before, $T \otimes B$ integral is evaluated analytically and the result is found as:

$$T \otimes B = (a_0 + a_1u + a_2u^2 + a_3u^3)(b_0 + b_1v) \quad (5.17c)$$

Therefore in order to evaluate the second integral in (5.17b) analytically, one needs to evaluate the integral of $1/R$ with multiplicative terms $[1 \ u \ u^2 \ u^3]$ and $[1 \ v]$. These integrals are given in [32] and they are used when developing the software code.

5.1 Numerical Results

While developing the software code, a step-by-step procedure is applied. First the admittance matrix is calculated and its accuracy is verified. As a verification example, dipole antennas standing in free space is considered. First the mutual coupling between two dipoles with different lengths is considered then the input impedance of a dipole is calculated to check the accuracy of singularity extraction procedure.

Current distribution on a dipole with dimensions $L \times W$, is assumed to be sinusoidal in the following form:

$$e_x^a = \frac{\text{sink}_e(\frac{L}{2} - |y|)}{W\text{sink}_e L/2} \quad (5.18)$$

Therefore the amplitude of each rooftop function is determined according to this sinusoidal distribution as shown in Figure 5.2.

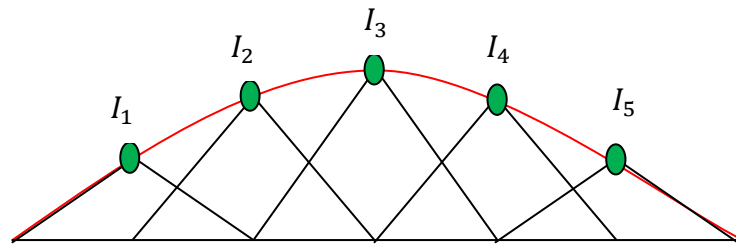


Figure 5. 2 Sinusoidal Current Distribution on the Slot with Meshes.

5.1.1 Mutual Impedance Calculation

Mutual impedance between two dipoles in free space exists in the literature. Therefore, in order to check if Y^e term is calculated accurately or not, two dipoles are created and sinusoidal current distribution on these dipoles are assumed. At the configuration, seen in Figure 5.3, two dipoles are placed along x-direction and they are separated by distance, d , in y-direction.

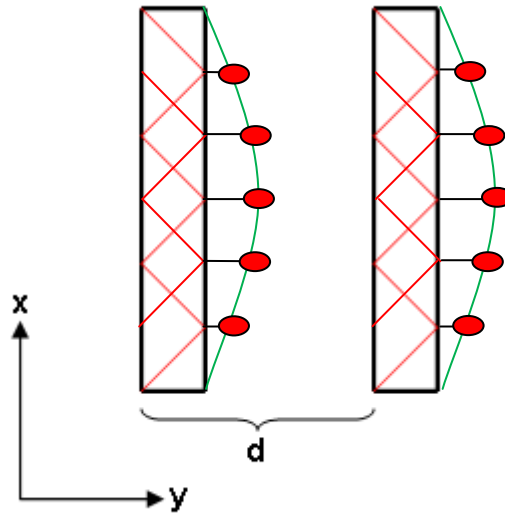


Figure 5. 3 Calculation of the Mutual Coupling Between Two Dipoles.

Admittance matrix is calculated and the mutual coupling is calculated from the matrix product given below:

$$\text{Mutual Coupling} = [I]^T [Y^e] [I] \quad (5.19)$$

For different dipole lengths, the variation of mutual impedance with respect to d are presented and compared to the results found in literature [33], as seen in Figure 5.4.

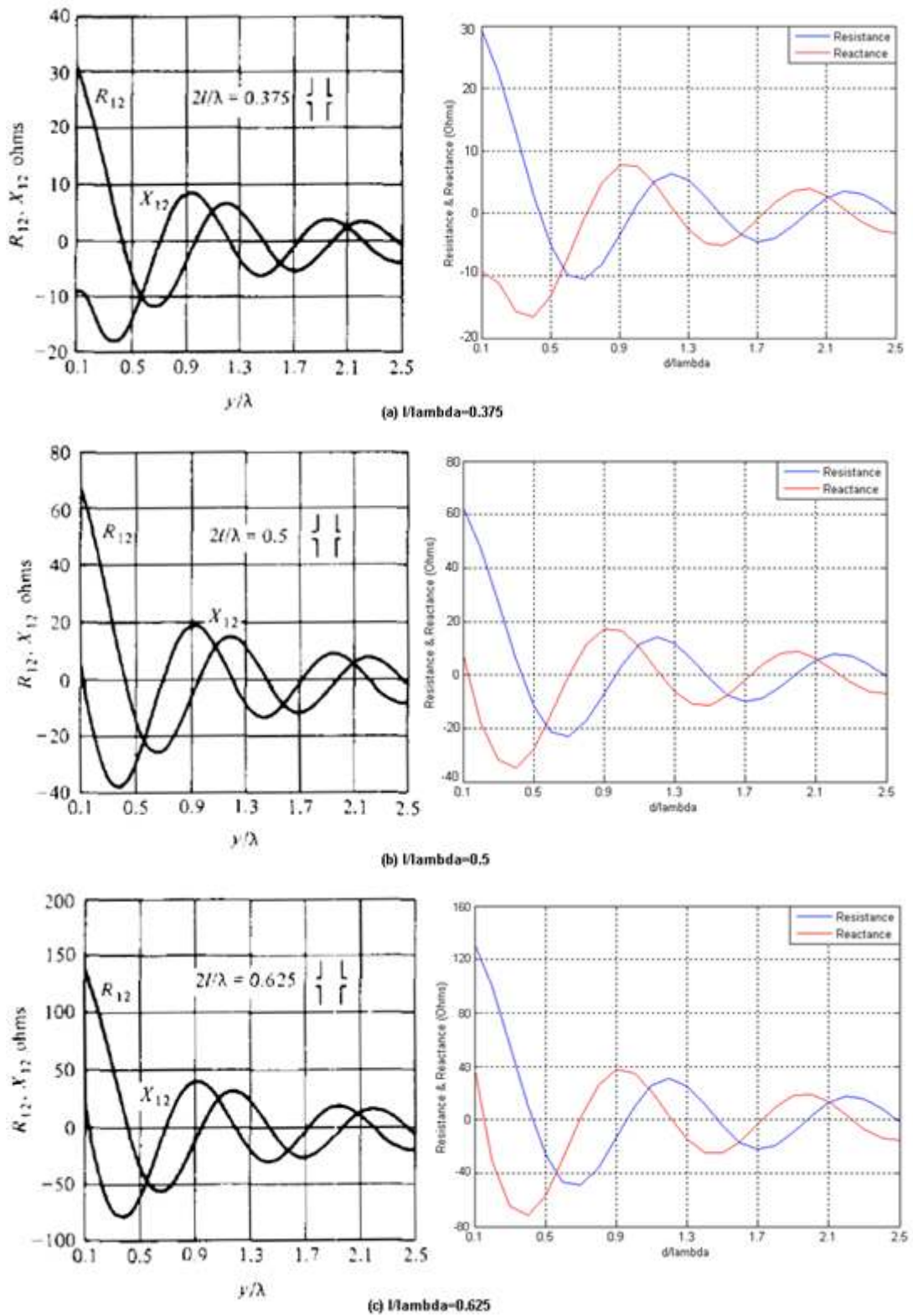


Figure 5. 4 Comparisons of the Mutual Impedance Characteristics of Two Dipoles with a Variation of the Distance Between Slots.

As seen from the Figure 5.4, a good agreement with the reference results is achieved.

5.2 Self Impedance Calculation of the Dipole

After the verification of the mutual impedance between two dipoles is completed by comparing the results with the literature, this section includes the calculation of the self impedance of the dipole. Singularity extraction method will also be verified with this example.

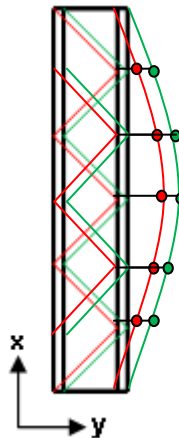


Figure 5. 5 Calculation of the Self Impedance of the Dipole.

As seen in Figure 5.5, self impedance of the dipole is calculated similar to the calculation of mutual impedance of the two dipoles. The difference is that the separation of the two dipoles in y-direction, d , is set to zero. Therefore, two dipoles are overlapped and the same code can be used to calculate the self impedance of the dipole.

In order to check the accuracy of the obtained result, it is compared with the data in the literature, with [33], by varying the length of the dipole. Comparison results can be seen in Figure 5.6.

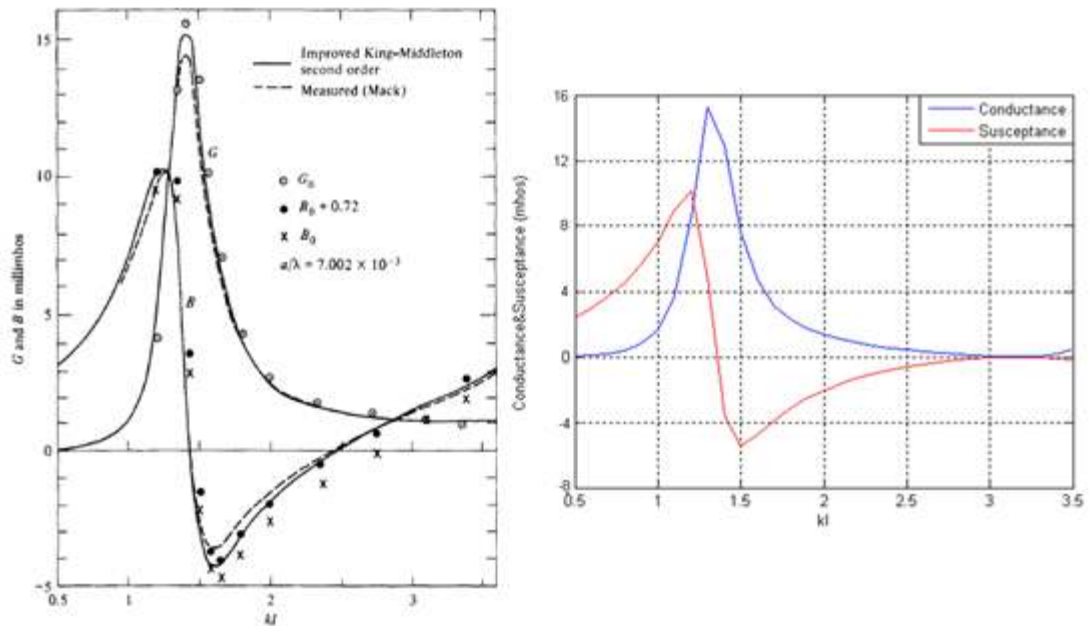


Figure 5. 6 Comparison of the Self Impedance of the Dipole.

As seen from Figure 5.6, the characteristics of the self impedance of a dipole resemble each other. The differences might be due to the sinusoidal current distribution assumption.

5.3 Results about Rectangular and H-shaped Slots

Impedance of the slot can be calculated by applying the method presented in this chapter. First, the impedance of a rectangular slot is calculated and compared with the data in the literature [30]. Comparisons are given for a slot on the ground plane of a microstripline with a dielectric constant of 2.2, thickness of 1.6cm, slot length of 4.02cm, slot width of 0.07cm and feed line width of 0.5cm.

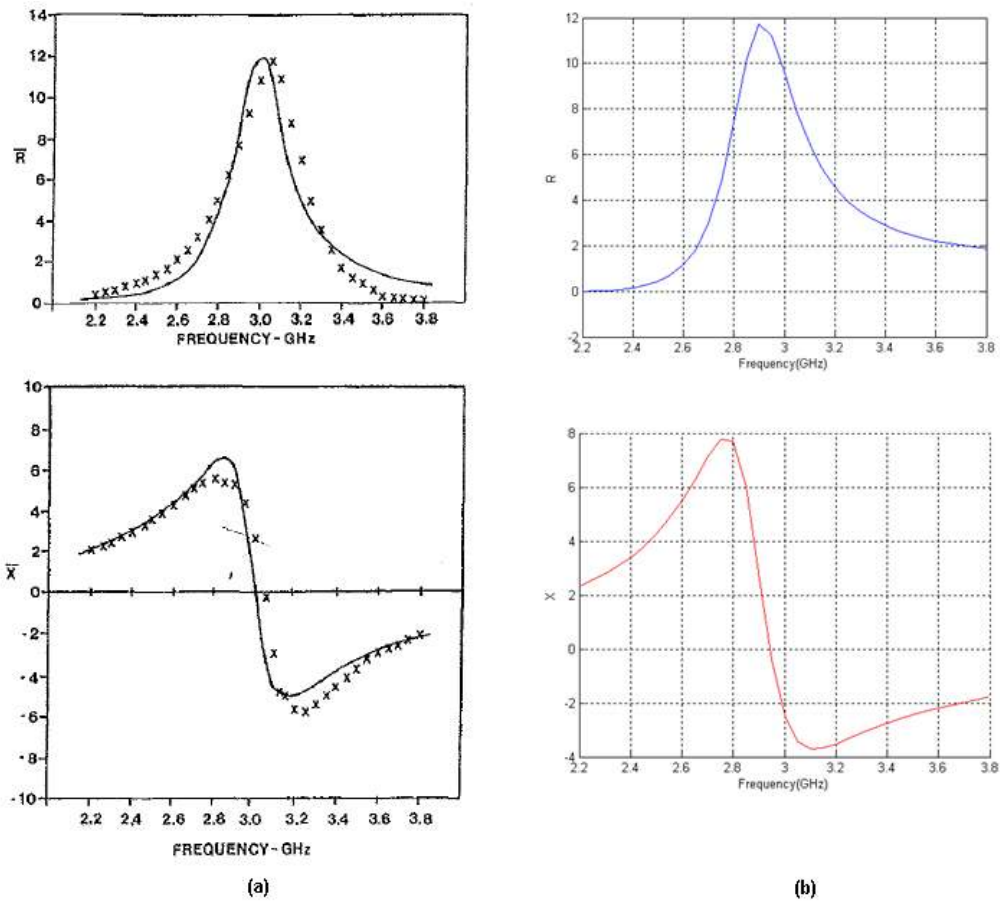


Figure 5.7 Impedance Comparison of a Slot in the Ground Plane of a Microstripline (a) Results from [30], solid line:theory, x: measurement (b) Result from Equations above.

It is seen from Figure 5.7 that there is a slight difference between the resonance frequencies of the slots. The approach proposed in [30] is utilized in this thesis. However, there is a considerable difference in the application of the method. In [30] the spectral domain formulation is used, whereas the spatial domain formulation is preferred in this thesis. Therefore, the discrepancy might be due to the errors introduced by the DCIM method.

Next, H-shaped slots are studied. For rectangular slots, only magnetic currents along the length of the slot are considered. For H-shaped slots, full-wave analysis are performed to investigate whether magnetic current components that are perpendicular to the center slot need to be included to model the H-shaped slot accurately. Therefore, the electric field distributions on rectangular and H-shaped

slots are calculated by a Finite Element Method based electromagnetic simulation software (HFSS by Ansoft) and the results are presented in Figure 5.8. According to Figure 5.8, fields lying perpendicular to the slot length are much stronger than the fields lying parallel to the slot length. In the light of this observation, impedances of the slots are calculated by considering only the field components that are perpendicular to the length of the slot (or magnetic current components along the slot).

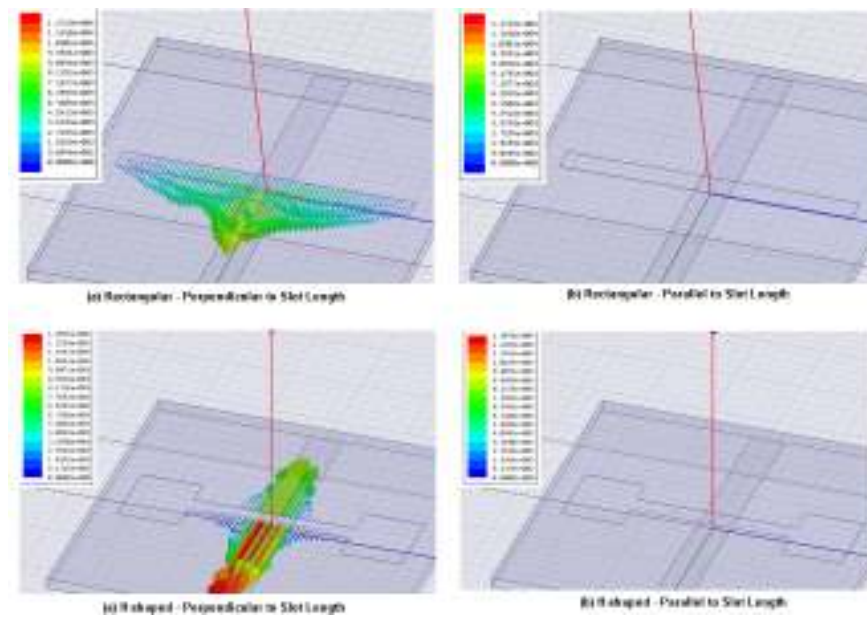


Figure 5. 8 Electric Fields for Rectangular and H-shaped Slots

H-shaped slot is divided into subdomains and the magnetic current on the slot is expanded in terms of only y-directed basis functions as shown in Figure 5.9.

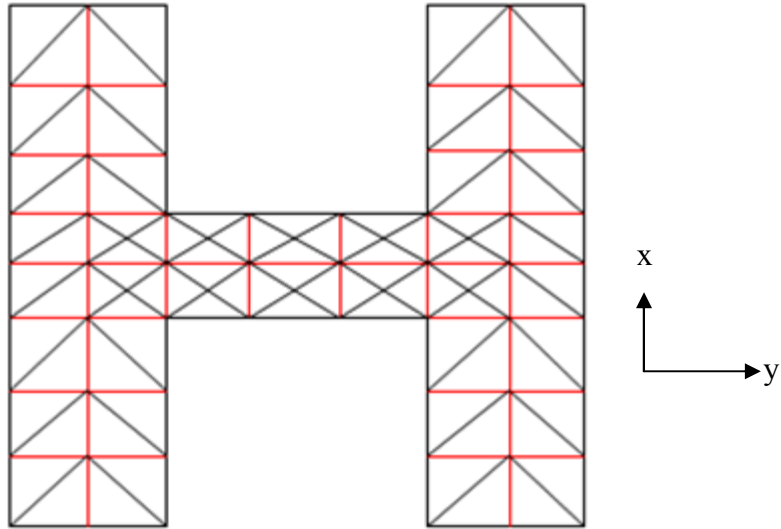


Figure 5. 9 Meshing the H-shaped slot

Slot impedance for an H-shaped slot is calculated in MATLAB from the equations described above and comparison of this impedance with impedance found in CST Microwave Design Studio is done. Dielectric substrate used in the analysis phase has a dielectric constant of 2.5 and thickness of 0.16cm. In addition, feed line width is 0.5cm. Length of the center slot is taken as 3.84cm, width of the slot is taken as 0.07cm, length of the slot edge is taken as 1.6cm and width of the slot edge is taken as 0.09cm. Real and imaginary parts of the slot impedances are given in Figure 5.10.

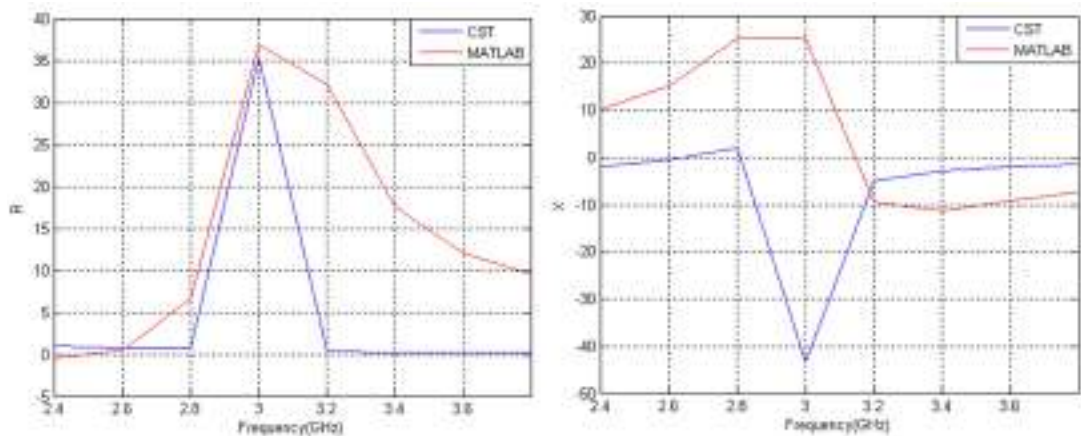


Figure 5. 10 Modeling and Simulation Comparison for an H-Shaped Slot.

It can be observed from Figure 5.10 that although there is not a perfect agreement between the simulation results and the results of the equivalent circuit model, the

equivalent circuit model could at least estimate the resonance frequency quite accurately. The discrepancy may be due to neglecting the magnetic current components in the x-direction. Especially as the length of the edge slots get larger, x-directed currents become more effective. Hence, as future work, x-directed currents will be included in the formulation in order to model the H-shaped slot more accurately.

CHAPTER 6

CONCLUSION

This thesis includes the design of a wideband dual-polarized microstrip antenna and equivalent circuit modeling of the H-shaped slot for aperture-coupled microstrip antennas. At the design phase of antenna, aperture-coupled configuration is selected to meet the wideband requirement. Step by step improvement is done at the design of the antenna. At the beginning, studies are done on the rectangular slotted aperture-coupled microstrip antenna and this antenna is designed to respond 20% bandwidth requirement. Parametrical analyses are carried out and effects of each variation on the antenna parameters, such as resonance frequency, bandwidth and input impedance, are observed. According to the results of these analyses, design of an aperture-coupled microstrip antenna with a 20% bandwidth is achieved. However, length of the slot on the aperture is so large that this prevents this antenna to be used in applications that require dual polarization operation. Next, to decrease the length of the slot, aperture coupled antenna with H-shaped slot is considered. Parametrical analyses are done with H-shaped slotted antenna and effects of each parameter on antenna performance are investigated. Then, an antenna with H-shaped slot is designed that provides 20% bandwidth. It is observed that the same bandwidth is achieved for the rectangular and H-shaped slots, but the slot is shorter in the H-shaped configuration. Later, studies are done in dual-polarization operation. Same antenna performance is tried to be achieved for both polarizations. At this stage, coupling between two slots have to be as small as possible. After the design process of the antenna is completed, antenna with determined parameters are produced and measured. The measurement results of the designed antenna indicate

that the antenna exhibits 20% bandwidth with center frequency at 9.5GHz and the coupling between two ports of the antenna is smaller than -20dB. These measurement results verify the simulation results obtained by CST Microwave Studio®.

At the second part of this thesis, equivalent circuit modeling of the H-shaped slot fed with an infinite microstrip line is studied. The slot can be modeled as a series impedance and the aim at this part was to calculate this equivalent impedance of the slot. For this aim, a reciprocity theorem based method, which was originally proposed to analyze rectangular slots, is generalized for H-shaped slots. The formulation is implemented in the spatial domain and DCIM is utilized to calculate the Green's functions in the spatial domain. A software code is developed in MATLAB. First, the impedance values calculated with this code and the results found in literature are compared for rectangular slots, they are in good agreement. Then, H-shaped slots are analyzed and the computed values are compared with the simulation results obtained from CST Microwave Studio. It is observed that although the resonance frequency of the slot can be predicted quite accurately, the magnetic currents flowing along the edge slots should also be included in the formulation in order to model the H-shaped slot more accurately. This extension is planned as a future work.

In addition to that, in the future, the developed code can be used to analyze and design series fed H-shaped slot antenna arrays including the mutual coupling effects between the slots. Moreover, the developed code can be extended for the equivalent circuit modeling of aperture coupled patch antennas with arbitrary slot shapes. The equivalent circuit of an aperture coupled antenna consists of a transformer and two impedance values connected in parallel at the secondary side of the transformer. One of the impedance models the slot and the other one models the patch antenna. By using the developed code, turn ratio of the transformer and the impedance of the slot can be calculated. Therefore, only an extension to calculate the impedance of the antenna will be needed.

APPENDIX

Coefficient Calculation in x-direction

Slot is divided into triangular meshes and electric field is found by calculating the integral of the multiplication of triangles. At the beginning of the calculation, equations of test and base half triangles are defined in Figure A.1.

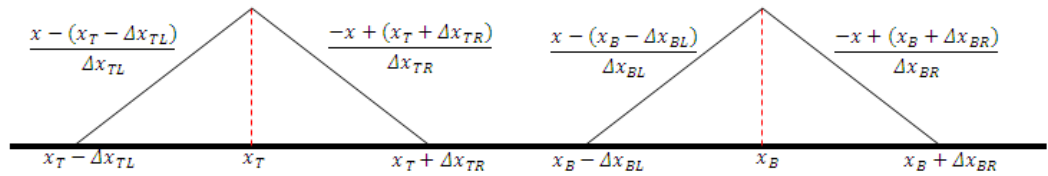


Figure A. 1 Half Triangle Equations of Test and Base Triangles.

Coefficients in x-direction are calculated by taking the convolution of the test and base half triangles in left-left, left-right, right-left and right-right cases of base-test half triangles respectively shown in Figure A.2.

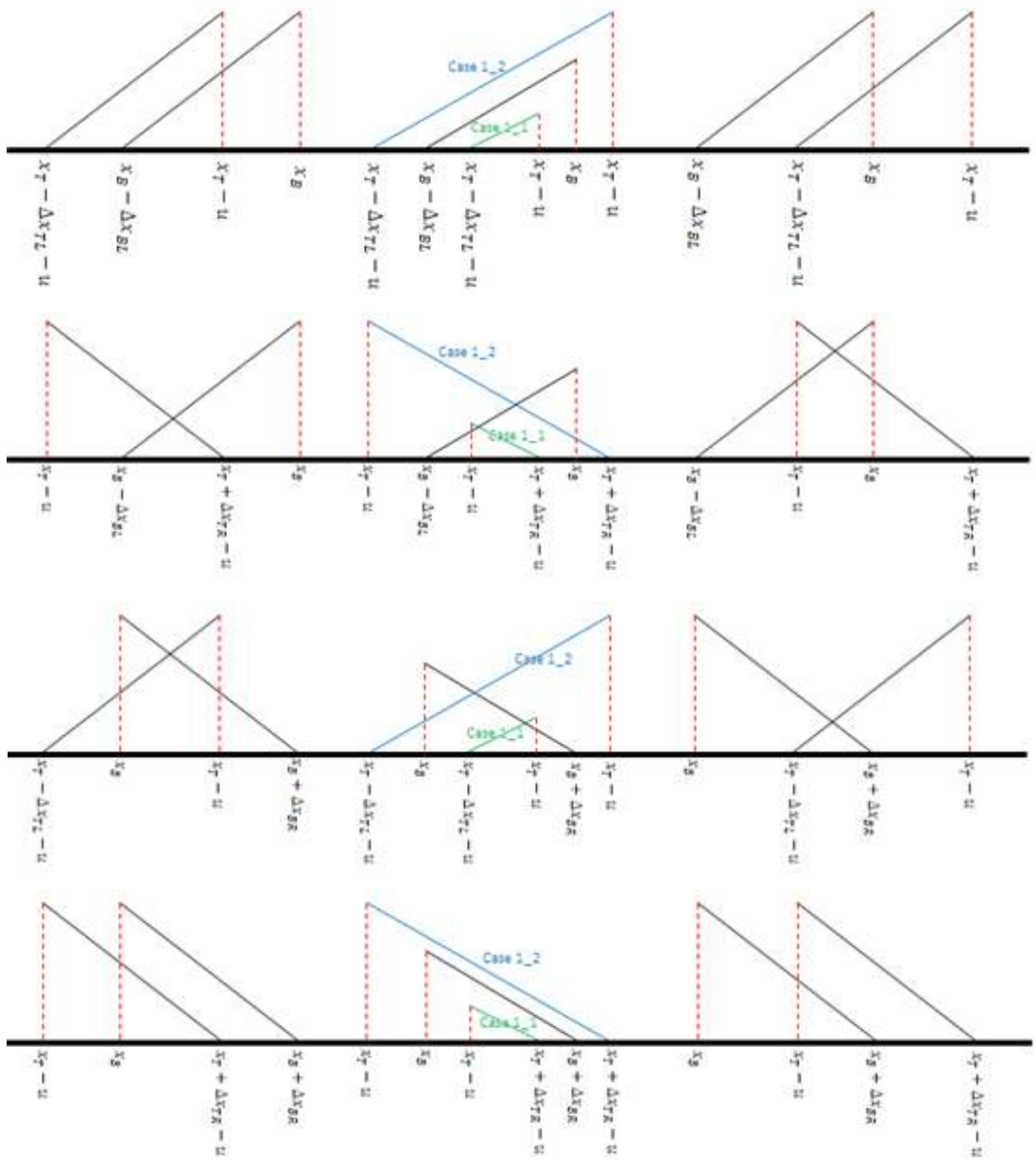


Figure A. 2 Situations for the Convolution of Test and Base Half Triangles (a) left-left case, (b) left-right case, (c) right-left case, (d) right-right case.

Convolution of the test and base triangles are taken from the formula A.1 in x-direction.

$$\int T(u + x')B(x')dx' \tag{A.1}$$

Coefficients in front of u^n is calculated and put in a matrix variable in order to use in triangle convolution.

Triangle Convolution in x-direction

After calculating the coefficients for the cases of the convolution of test and base half triangles, convolution of the test and base triangles are calculated by using the coefficients found above. New situations for the two triangle convolution and integral limits are determined for each case. Cases are shown in Figure A.3.

$dx \quad il < dx \quad bl$

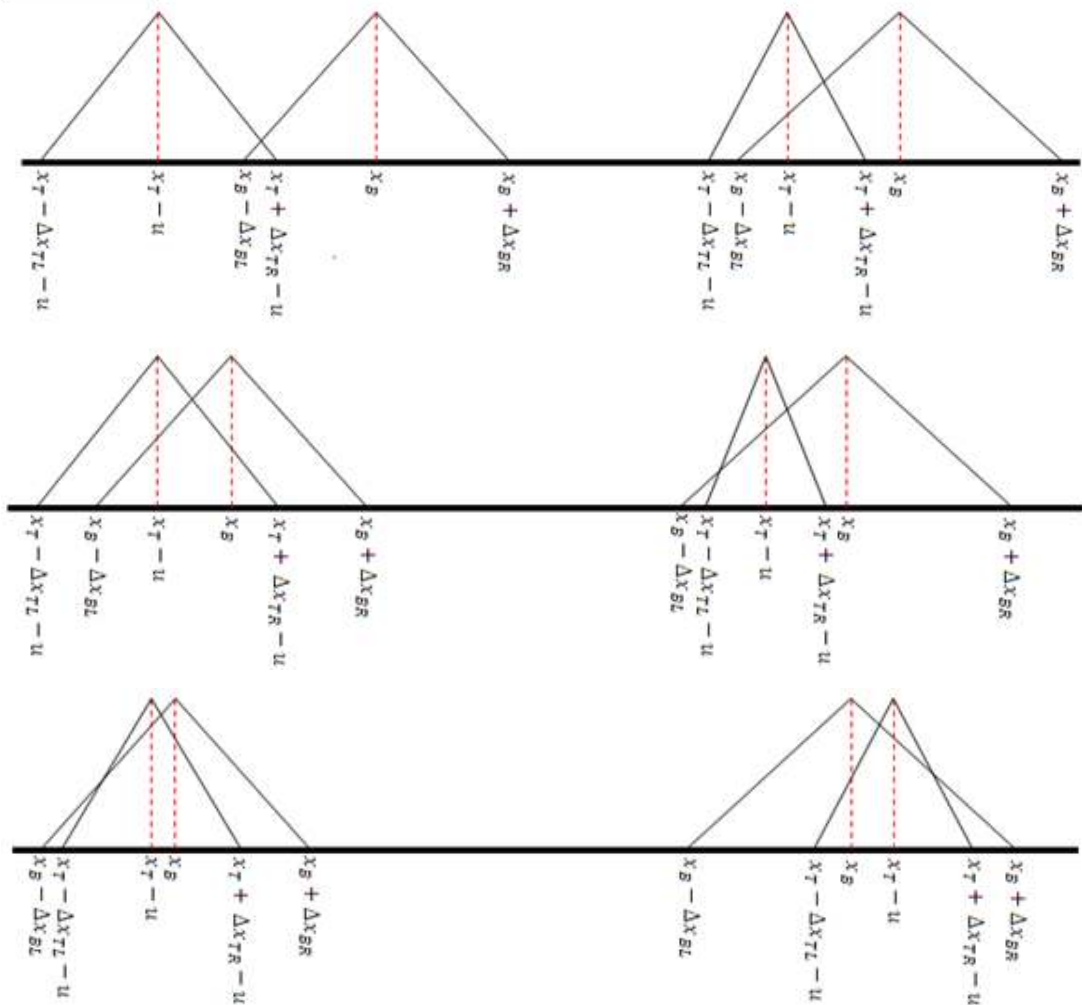
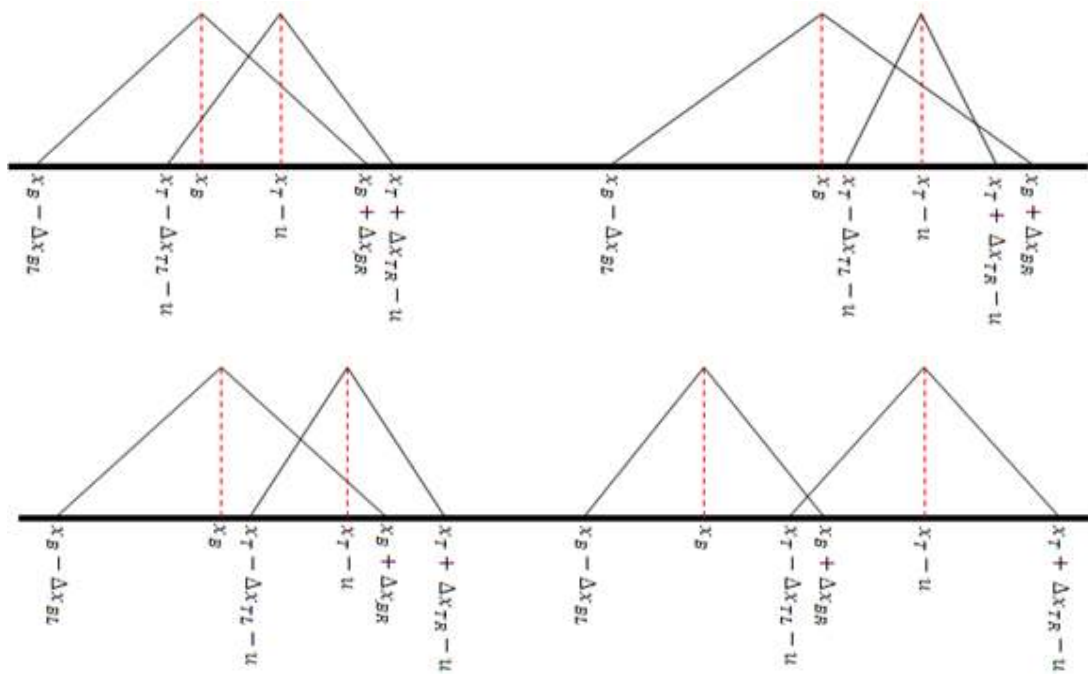


Figure A. 3 Cases for the Convolution of Test and Base Triangles for all Situations.



$dx_{TL} > dx_{BL}$

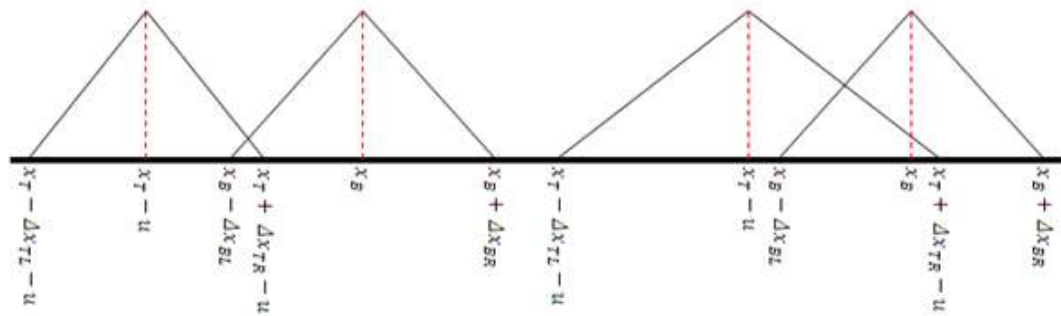


Figure A.3 Cases for the Convolution of Test and Base Triangles for all Situations (cont'd).

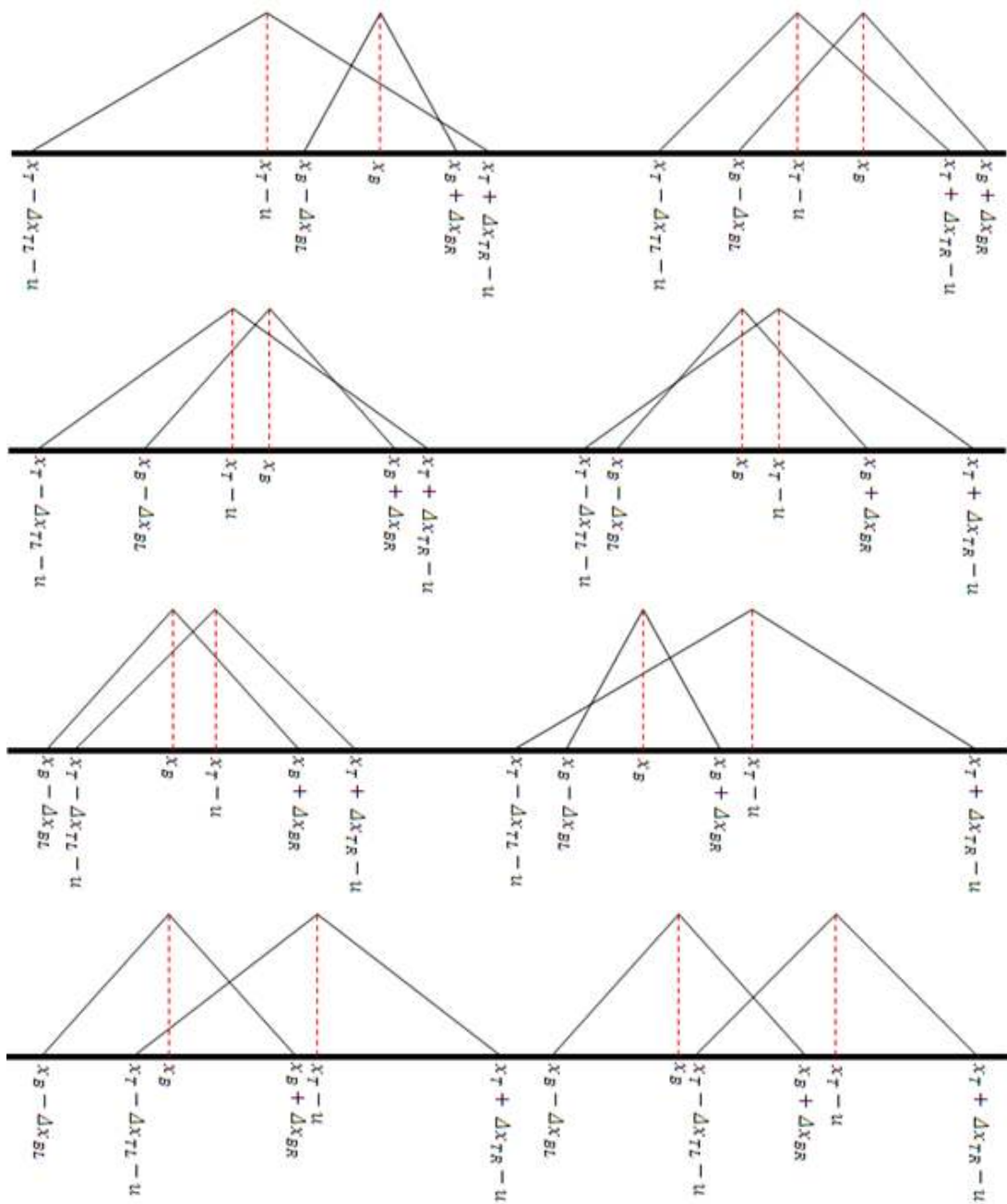


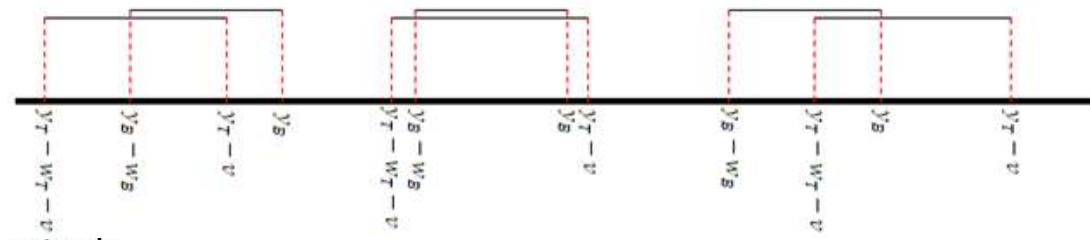
Figure A.3 Cases for the Convolution of Test and Base Triangles for all Situations (cont'd).

Step Function Convolution in y-direction

In two dimensional views, if triangle is seen at the x-direction, step function is observed at the y-direction. In order to find the coupling of the two triangles, it is necessary to calculate the movement of the triangles in y-direction. Therefore,

coefficients must be computed by calculating the convolution. Likewise the triangle convolution in x-direction, step functions is multiplied by moving one of the functions, test function, in y-direction with assuming base function is stable. Convolution of the test and base functions in y-direction are found by solving the convolutions given in Figure A.4.

$w_t > w_b$



$w_t < w_b$

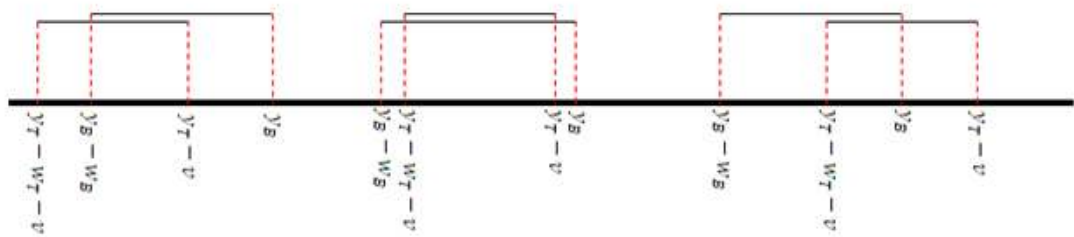


Figure A. 4 Cases for the Convolution of Test and Base Functions in y-direction for all Situations.

Integrals for Charge Functions

At the equation of mutual coupling, convolution of the derivation of the test and base triangles are required. Derivative of the triangular functions are step functions. Therefore, derivative of the triangles in sections above are found and integrals of the convolutions of these step functions are calculated for all situations. Integral limits are the same as the triangular convolutions. All the cases of the derived triangular convolutions are given in Figure A.5.

$dx_{tl} < dx_{bl}$

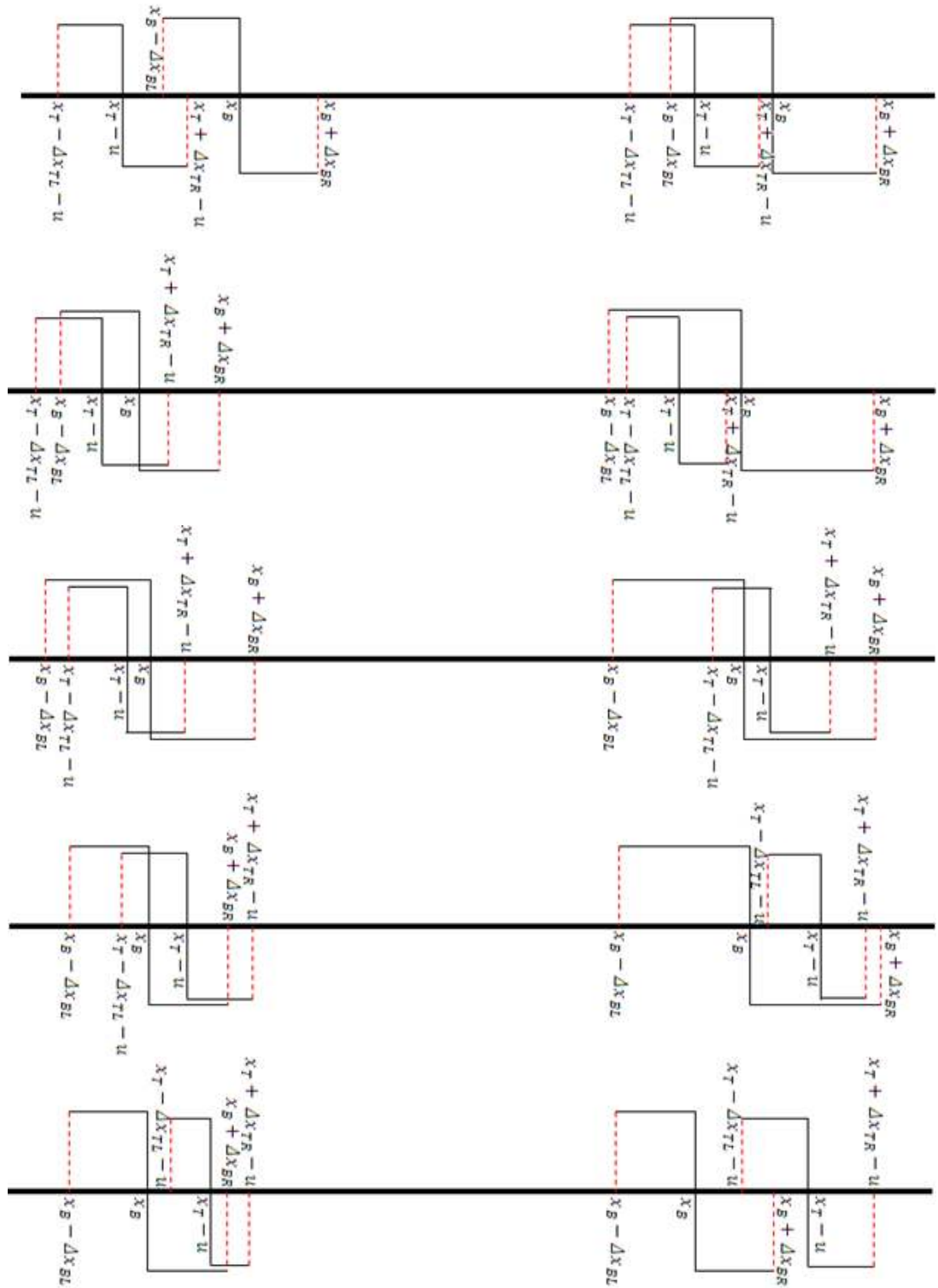


Figure A. 5 Cases for the Convolution of the Derivatives of Test and Base Functions for all Situations.

$dx_{tl} > dx_{bl}$

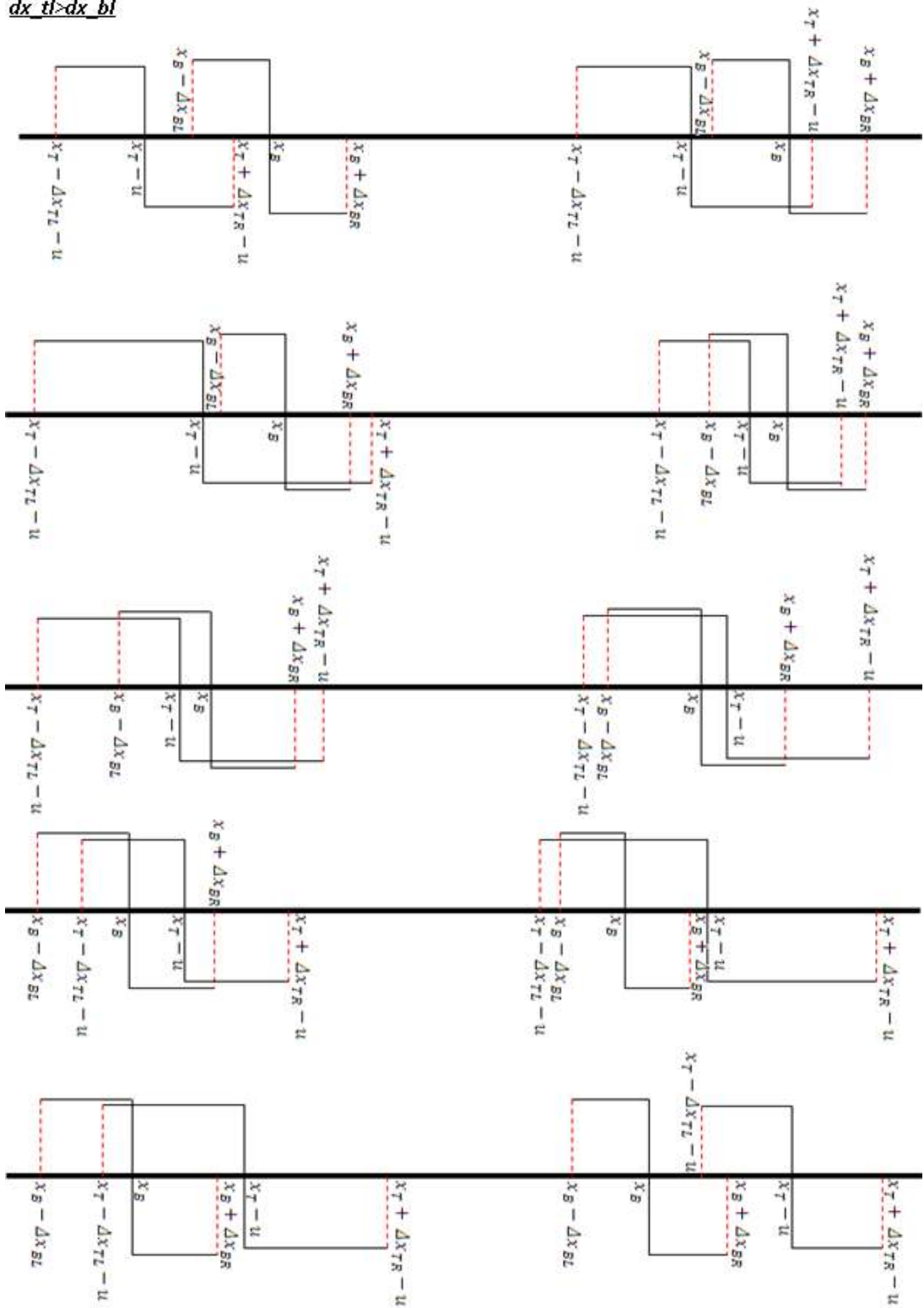


Figure A.5 Cases for the Convolution of the Derivatives of Test and Base Functions for all Situations (cont'd).

REFERENCES

- [1] C. A. Balanis, "Antenna Theory Analysis and Design Second Edition", John Wiley & Sons, United States of America, 1997.
- [2] R. Garg, P. Bhartia, I. Bahl and A. Ittipoon, "Microstrip Antenna Design Handbook", Artech House, Boston, London, 2001.
- [3] I. J. Bahl and P. Bhartia, "Microstrip Antennas", Artech House, Dedham, Massachusetts, 1980.
- [4] J. R. James and P. S. Hall, "Handbook of Microstrip Antennas", Peter Peregrinus Ltd., London, United Kingdom, 1989.
- [5] S. D. Targonski, R. B. Waterhouse, and D. M. Pozar, "Design of Wide-Band Aperture-Stacked Patch Microstrip Antennas", IEEE Trans. on Antennas and Propagation, Vol. 46, No. 9, September 1988.
- [6] Tzung-Wern Chiou and Kin-Lu Wong, "A Compact Dual-Band Dual-Polarized Patch Antenna for 900/1800-MHz Cellular Systems", IEEE Trans. on Antennas and Propagation, Vol. 51, No. 8, August 2003.
- [7] D. M. Pozar, "A Review of Aperture Coupled Microstrip Antennas: History, Operation, Development, and Applications", Amherst, MA 01003, May 1996.
- [8] H. S. Shin and N. Kim, "Wideband and High-Gain One-Patch Microstrip Antenna Coupled with H-Shaped Aperture", Electronics Letters, Vol.38, No.19, pp.1072-1073, September 2002.

- [9] Steven (Shichang) Gao, "Dual-Polarized Broad-Band Microstrip Antennas Fed by Proximity Coupling", IEEE Trans. on Antennas and Propagation, Vol. 53, No. 1, January 2005.
- [10] Shi-Chang, Le-Wei Li, Mook-Seng Leong and Tat-Soon Yeo, "Wide-Band Microstrip Antenna with an H-Shaped Coupling Aperture", IEEE Trans. on Vehicular Technology, Vol. 51, No. 1, January 2002.
- [11] Steven Mestdagh and Guy A. E. Vandenbosch, "A Parameter Study of Aperture-Coupled CPW-Fed Stacked Microstrip Antennas", K. U. Leuven, Belgium.
- [12] Kin-Lu Wong, Hao-Chun Tung and Tzung-Wern Chiou, "Broadband Dual-Polarized Aperture-Coupled Patch Antennas with Modified H-Shaped Coupling Slots", IEEE Trans. on Antennas and Propagation, Vol. 50, No. 2, February 2002.
- [13] K. Chemachema and A. Benghalia, "Input Impedance Calculation for Coax-Fed Rectangular Microstrip Antenna with and without Airgaps Using Various Algorithms", PIERS Proceedings, Marrakesh, MOROCCO, March 20-23 2011.
- [14] D. D. Sandu, O. Avadanei, A. Ioachim, G. Banciu and P. Gasner, "Microstrip Patch Antenna with Dielectric Substrate", Journal of Optoelectronics and Advanced Materials, Vol.5, No.5, 2003, p.1381-1387.
- [15] Wayne S. T. Rowe and Rod B. Waterhouse, "Investigation Into the Performance of Proximity Coupled Stacked Patches", IEEE Trans. on Antennas and Propagation, Vol.54, No.6, June 2006.
- [16] Jibendu Sekhar Roy and Milind Thomas, "Investigations on a New Proximity Coupled Dual-Frequency Microstrip Antenna for Wireless Communication", Mikrotalasna Revija, June 2007, p. 12.

- [17] M. A. Saed, "Reconfigurable Broadband Microstrip Antenna Fed by a Coplanar Waveguide", *Progress in Electromagnetics Research, PIER* 55, 2005, p.227-239.
- [18] M. Irsadi Aksun, Shun-Lien Chuang and Yuen Tze Lo, "On Slot-Coupled Microstrip Antennas and Their Applications to CP Operation-Theory and Experiment", *IEEE Trans. on Antennas and Propagation*, Vol. 38, No. 8, August 1990.
- [19] Zarreen Aijaz and S. C. Shrivastava, "An Introduction of Aperture Coupled Microstrip Slot Antenna", *International Journal of Engineering Science and Technology*, Vol. 2(1), 2010, p. 36-39.
- [20] Yıldırım Meltem, "Design of Dual Polarized Wideband Microstrip Antennas", Msc. Thesis, METU, 2010.
- [21] Anil B. Nandgaonkar and Shankar B. Deosarkar, "Broadband Stacked Patch Antenna for Bluetooth Applications", *Journal of Microwaves, Optoelectronics and Electromagnetic Applications*, Vol. 8, No. 1, June 2009.
- [22] D. K. Srivastava, J. P. Saini and D. S. Chauhan, "Broadband Stacked H-Shaped Patch Antenna", *International Journal of Recent Trends in Engineering*, Vol. 2, No. 5, November 2009.
- [23] Naser Ghassemi, Shahram Mohanna, J. Rashed-Mohassel and M. H. Neshati, "A UWB Aperture Coupled Microstrip Antenna for S and C Bands", 4th IEEE International Conference on Wireless Communication, Networking and Mobile Computing, Dalian, China, October 12-14, 2008.
- [24] N. Ghassemi, J. Rashed-Mohassel, M. H. Neshati and M. Ghassemi, "Slot Coupled Microstrip Antenna for Ultra Wideband Applications in C and X Bands", *Progress in Electromagnetics Research M.*, Vol. 3, p. 15-25, 2008.

- [25] Sami Hienonen, Arto Lehto, Antti V. Raisanen, "Simple Broadband Dual-Polarized Aperture-Coupled Microstrip Antenna", IEEE Antennas and Propagation Society International Symposium, Vol. 2, p. 1228-1231, 11-16 July, 1999.
- [26] Rashid A. Saeed and Sabira Khatun, "Design of Microstrip Antenna for WLAN", Journal of Applied Sciences, Vol. 5(1), p. 47-51, 2005.
- [27] Pinaki Mukherjee and Bhaskar Gupta, "Genetic Algorithm-Based Design Optimisation of Aperture-Coupled Rectangular Microstrip Antenna", Defence Science Journal, Vol. 55, No. 4, p. 487-492, October 2005.
- [28] Zarreen Aijaz and S. C. Shrivastava, "Coupling Effects of Aperture Coupled Microstrip Antenna", Internal Journal of Engineering Trends and Technology, July-August Issue 2011.
- [29] Tanushree Bose and Nisha Gupta, "Neural Network Model for Aperture Coupled Microstrip Antenna", Microwave Review, September 2008.
- [30] David M. Pozar, "A Reciprocity Method of Analysis for Printed Slot and Slot-Coupled Microstrip Antennas", IEEE Trans. on Antennas and Propagation, Vol. AP-34, No. 12, December 1986.
- [31] Levent Gürel and Özgür Ergül, "Singularity of the Magnetic-Field Integral Equation and Its Extraction", IEEE Antennas and Wireless Propagation Letters, Vol.4, 2005.
- [32] Alatan Hayırlıoğlu Lale, "Use of Computationally Efficient MoM in the Analysis and Design of Printed Structures", PhD. Thesis, METU, 1997.
- [33] Robert S. Elliot, "Antenna Theory and Design Revised Edition", John Wiley & Sons, United States of America, 2003.
- [34] David B. Davidson, "Computational Electromagnetics for RF and Microwave Engineering", Cambridge University Press, New York, 2005.

- [35] Aytaç Alparslan, M. I. Aksun and Krzysztof A. Michalski, “Closed-Form Green’s Functions in Planar Layered Media for All Ranges and Materials”, IEEE Transactions on Microwave Theory and Techniques, Vol. 58, No. 3, March 2010.
- [36] S. Maci, L. Borselli, G. Avitabile, G. Biffi Gentili and R. Tiberio, “A CAD-Oriented Approach for Aperture-Coupled Patch Antennas”, International Journal of Microwave and Millimeter-Wave Computer-Aided Engineering, Vol. 3, No. 4, 386-396 (1993).
- [37] Mikael Dich, Allen Østergaard and Ulrich Gothelf, “A Network Model for the Aperture Coupled Microstrip Patch”, International Journal of Microwave and Millimeter-Wave Computer-Aided Engineering, Vol. 3, No. 4, 326-339 (1993).
- [38] İncebacak Mustafa, “Desing of Series-Fed Printed Slot Antenna Arrays Excited by Microstrip Lines”, Msc. Thesis, METU, 2010.